



The present work was submitted to
the Faculty of Raw Materials and Environmental Engineering,
German-Mongolian Institute for Resources and Technology

ASSESSMENT OF CLIMATE AND VEGETATION CHANGES IN SOME AREAS OF THE MONGOLIAN PLATEAU USING SATELLITE DATA

Bachelor's Thesis

By

URANGO Baasandorj

Study program: Environmental Engineering

Student ID: B2100598

1st Supervisor/Examiner: Prof. Dr. Gantuya Ganbat

2nd Supervisor/Examiner: MSc. Nandin-Erdene Geserbaatar

Ulaanbaatar/Nalaikh

2025

Statutory Declaration

Urangoo, Baasandorj

B2100598

Last Name, First Name

Student ID Number

I hereby affirm in lieu of an oath that I provided the submitted bachelor thesis

ASSESSMENT OF CLIMATE AND VEGETATION CHANGES IN SOME AREAS OF THE MONGOLIAN PLATEAU USING SATELLITE DATA

I did not use any sources other than those stated. In case that the work is additionally submitted on a data medium, I declare that the written and the electronic form are completely identical. The work was not submitted in the same or similar form to any examination authority.

Ulaanbaatar/ Nalaikh 2025.05.28

Place, Date



Signature

Table of contents

Table of contents	2
Acknowledgement	3
List of Figures	4
List of Tables	5
Abstract	6
1. Introduction	7
1.1 Background study.....	7
1.2 Objective of the study.....	9
2. Methodology	9
2.1 Study Area.....	9
2.2 Satellite data sources and processing.....	12
2.3 Estimation of standardization and normalization.....	15
2.3.1 Normalization Process.....	15
2.3.2 Standardization Process.....	15
2.3.3 Thresholding and Conditioned Maps.....	16
2.4 Weight Determination Using Analytic Hierarchy Process (AHP).....	17
2.5 Classification of vegetation-climate response type analysis.....	19
3. Results and Discussion	21
3.1 NDVI and LST mapping from 2000 to 2024.....	21
3.2 Estimation of ET using NDVI and LST.....	22
3.3 Calculation of the normalized climate and vegetation Index.....	23
3.4 Calculation of the standardized climate and vegetation index.....	26
3.5 Weighted integration of parameters using Pair-Wise Comparison method.....	28
3.5.1 Parameter Relationship and Conceptual Ordering.....	28
3.5.2 Development and Evaluation of Comparison Matrices.....	28
3.6 Regional analysis of vegetation–climate response types.....	31
3.6.1 Transboundary desert regions: Southern Mongolia and Inner Mongolia.....	31
3.6.1.1 Normalized composite map results.....	31
3.6.1.2 Standardized composite map results.....	32
3.6.1.3 Classification of vegetation–climate response types.....	33
3.6.2 Transboundary steppe and regions: Eastern Mongolia and Inner Mongolia.....	36
3.6.2.1 Normalized composite map results.....	36
3.6.2.2 Standardized composite map results.....	37
3.6.2.3 Classification of vegetation–climate response types.....	38
3.6.3 Northern regions of Mongolia: Selenge and Darkhan provinces.....	40
3.6.3.1 Normalized composite map results.....	41
3.6.3.2 Standardized composite map results.....	42
3.6.3.3 Classification of vegetation–climate response types.....	43
4. Recommendation based on regional analysis of vegetation–climate response types ..	45
5. Conclusion	46
References	48
Appendix	51

Acknowledgement

First and foremost, I would like to express my sincere gratitude to Prof. Dr. Gantuya Ganbat, for her expert guidance, continuous encouragement, and valuable academic insights throughout this research. Her thoughtful feedback and unwavering support have been essential to the successful development of this thesis.

I am also deeply thankful to MSc. Nandin-Erdene Geserbaatar, for her dedicated assistance and practical help, especially in the QGIS-based spatial analysis. Her support in handling geospatial data and analytical tools significantly contributed to the technical foundation of this study.

I would like to extend my appreciation to the Faculty of Raw Materials and Environmental Engineering at the German-Mongolian Institute for Resources and Technology (GMIT) for providing the academic environment, resources, and opportunities that made this research possible.

I am truly grateful to my family for their constant love, patience, and encouragement throughout my academic journey. Their belief in me has been my greatest source of strength.

Finally, I thank my friends and fellow students for their support, collaboration, and shared learning experiences, which made this journey both enriching and memorable.

List of Figures

Figure 1. Satellite data processing and ET estimation workflow.....	13
Figure 2. Workflow for standardizing and normalizing NDVI, LST, ET.....	17
Figure 3. Classification of Vegetation–Climate Response Types based on Normalized and Standardized Composite Indices.....	19
Figure 4. Mean NDVI of July 2000.....	20
Figure 5. Mean LST of July 2000.....	20
Figure 6. Mean NDVI of May to August 2000.....	21
Figure 7. Mean LST of May to August 2000.....	21
Figure 8. Mean ET of July 2000.....	22
Figure 9. Sum ET of May to August 2000.....	22
Figure 10. Mean normalized NDVI of 2000-2024.....	24
Figure 11. Mean normalized ET of 2000-2024.....	24
Figure 12. Mean normalized LST of 2000-2024.....	24
Figure 13. Sum standardized NDVI (2000-2024).....	25
Figure 14. Sum standardized LST(2000-2024).....	25
Figure 15. Sum standardized ET (2000-2024).....	26
Figure 16. The order of the parameters.....	27
Figure 17. Standardized weighted map.....	29
Figure 18. Normalized weighted map.....	29
Figure 19. Normalized map of the transboundary desert region between southern Mongolia and Inner Mongolia.....	31
Figure 20. Standardized map of the transboundary desert region between southern Mongolia and Inner Mongolia.....	32
Figure 21. Vegetation–Climate Response Type Classification based on normalized and standardized composite values.....	33
Figure 22. Spatial distribution of response types across the transboundary desert region.....	34
Figure 23. Normalized map of the transboundary desert region between eastern Mongolia and Inner Mongolia.....	36
Figure 24. Standardized map of the transboundary desert region between eastern Mongolia and Inner Mongolia.....	37
Figure 25. Vegetation–Climate Response Type Classification of the transboundary steppe region between eastern Mongolia and Inner Mongolia.....	39
Figure 26. Spatial distribution map of vegetation-climate response types of the transboundary steppe region between eastern Mongolia and Inner Mongolia.....	40
Figure 27. Normalized map of the forest steppe regions of northern Mongolia.....	41
Figure 28. Standardized map of the forest steppe regions of northern Mongolia.....	43
Figure 29. Vegetation–Climate Response Type Classification of the forest steppe regions of northern Mongolia.....	44
Figure 30. Spatial distribution map of vegetation-climate response types of the forest steppe regions of northern Mongolia.....	46

List of Tables

Table 1. Soums of the transboundary desert region between southern Mongolia and Inner Mongolia, and the corresponding area.....9

Table 2. Soums of the transboundary steppe region between eastern Mongolia and Inner Mongolia, and the corresponding area.....10

Table 3. Soums of northern Mongolia (Selenge and Darkhan provinces), and the corresponding area.....11

Table 4. Normalization equation for each parameter.....14

Table 5. Standardization equation for each parameter.....15

Table 6. Thresholding conditions for standardized values.....16

Table 7. Saaty's fundamental scale.....16

Table 8. The value of the random consistency index.....17

Table 9. Variables and formulas used in AHP weight calculation.....18

Table 10. Minimum and maximum values of each parameter by the Mongolian Plateau.....23

Table 11. Summary of Consistency Metrics for Three Matrices.....27

Table 12. Chosen Pair-Wise Comparison Matrix.....28

Table 14. Vegetation–Climate Response Classification of Soums in Eastern Mongolia.....39

Table 15. Vegetation–Climate Response Classification of Soums in Northern Mongolia.....44

Abstract

The Mongolian Plateau is one of Central Asia's most climatically sensitive regions, where ecological changes driven by temperature rise, precipitation variability, and land-use pressure pose growing challenges for environmental sustainability. This study investigates long-term changes in vegetation and climate across three representative plateau regions, including the southern desert, the eastern steppe, and northern forest-steppe, using satellite-derived data from MODIS sensors (NDVI, LST, and ET) from 2000 to 2024. Data processing and analysis were conducted using Google Earth Engine and QGIS, applying normalization, standardization (Z-score), and weighted integration through the Analytic Hierarchy Process (AHP). A regional vegetation–climate response type classification was developed, dividing each study area into four types based on environmental conditions and interannual variability. Which are:

- Type I: high NDVI, low LST and ET, with low changes
- Type II: low NDVI, high LST and ET, with low changes
- Type III: high NDVI, low LST and ET, with high changes
- Type IV: low NDVI, high LST and ET, with high changes

In Umnugovi Province and neighboring areas of Inner Mongolia, Type I and Type IV accounted for 18.9% and 37.4% of the total area, respectively. In eastern Mongolia (Dornod and adjacent settlements), Type I and Type IV covered 28.8% and 34.0%, respectively. The northern regions (Selenge and Darkhan) exhibited smaller proportions of these types, with 5.0% for Type I and 19.3% for Type IV.

These classifications highlight the spatial heterogeneity in vegetation-climate responses under changing climatic conditions and emphasize the value of remote sensing data in informing regional environmental management, land-use policy, and climate adaptation strategies, particularly in mining-affected landscapes.

1. Introduction

1.1 Background study

The Mongolian Plateau (MP) is a vast ecological region dominated by natural grasslands, making it one of the most representative pastoral areas in the world. It is rich in grassland resources and supports extensive animal husbandry, which remains the primary mode of economic activity across much of the region. Geographically, the central expanse of the plateau spans Mongolia and the Inner Mongolia Autonomous Region of China, two territories that, while ecologically interconnected, are administered under different political systems and land management frameworks. [1]

Climate change has a profound impact on ecosystems worldwide, especially in regions where environmental conditions are inherently fragile and highly sensitive to climatic fluctuations. The Mongolian Plateau, being landlocked and surrounded by mountain ranges, experiences a harsh continental climate with sharp seasonal temperature and precipitation contrasts [2]. Its geographic isolation from oceanic influences results in low humidity and erratic weather patterns, which strongly affect regional vegetation dynamics and ecological resilience.

In recent decades, rising temperatures, altered precipitation regimes, and other climate-related stressors have significantly impacted both vegetation health and land cover patterns across Mongolia and the Inner Mongolian Autonomous Region of China. This region has become increasingly vulnerable to frequent extreme climatic events, including dzud winters characterized by severe cold, extensive snow cover, and livestock mortality, as well as prolonged summer droughts, both of which have intensified over the past decade [3].

According to the Mongolia Assessment Report on Climate Change (MARCC), the average annual temperature on the MP has increased at a rate of 0.23°C per decade, a higher rate than the 0.18°C observed across its four climatic sub-regions [4]. These warming trends, combined with seasonal and interannual climate variability, have placed additional pressure on the Plateau's grassland ecosystems, which are critical for local livelihoods and biodiversity conservation.

As of 2015, approximately 76.8% of the Mongolian national territory is degraded, primarily due to climate change and unsustainable land-use practices, such as overgrazing [5]. Inner Mongolia faces similarly severe challenges. Between the 1950s and 1980s, land degradation in Inner Mongolia intensified by 32%, primarily driven by overgrazing and land conversion, including the transformation of natural grasslands into agricultural fields, residential settlements, and industrial zones [6].

Ecosystem responses to extreme climate events vary significantly across the Mongolian Plateau, reflecting biome-specific differences in vegetation cover, land surface temperature (LST), and evapotranspiration (ET). [3, 7] These spatial variations in ecological sensitivity and resilience underscore the importance of regionally differentiated monitoring approaches in capturing the heterogeneity of climate impacts on land surface processes.

The long-term changes in climate and vegetation are evaluated based on various factors. To assess these changes, remote sensing data has become an invaluable tool. Satellite imagery and data obtained by remote sensing (RS) and geographical information systems (GIS) have enhanced our ability to notice intricate changes on the Earth's surface [8].

Over the past century, numerous vegetation indices have been developed using remotely sensed data, among which the Normalized Difference Vegetation Index (NDVI) remains the most widely used. NDVI has proven invaluable in monitoring vegetation status and detecting disturbances such as droughts, wildfires, floods, and frost events on regional to global scales [9,10].

Long-term studies have demonstrated that vegetation on the Mongolian Plateau is highly responsive to climatic variability. NDVI-based analyses have shown strong correlations between vegetation trends and changes in temperature and precipitation across the region [11]. In addition to climate factors, human activities such as overgrazing and land-use change also play a significant role in shaping vegetation dynamics [12].

NDVI is also a significant factor in estimating Land Surface Temperature (LST), as it directly influences land surface emissivity and is widely used in LST modeling [13]. LST is a fundamental geophysical variable for assessing surface radiation, heat, and moisture fluxes, as well as interactions with soil, vegetation, and anthropogenic structures. It provides insight into both natural ecosystem functioning and the impacts of land use [14].

According to the Intergovernmental Panel on Climate Change (IPCC), LST has increased across Asia, including the Mongolian Plateau, over the past century [15]. In this context, terrestrial evapotranspiration (ET), the process by which water is transferred from land surfaces to the atmosphere, serves as a critical component of the hydrological cycle and a key indicator of environmental change [16]. ET plays an essential role in monitoring climate impacts, evaluating rangeland health, and assessing water balance and vulnerability across ecosystems. Both NDVI and LST are closely linked to ET estimation. NDVI provides insight into vegetation cover and greenness, which influences transpiration rates, while LST is used in energy balance models to quantify latent heat flux. Studies have shown that NDVI trends are strongly associated with potential evapotranspiration patterns, making these parameters jointly valuable for understanding surface processes and climate-vegetation interactions [17].

ET levels on the Mongolian Plateau differ significantly across ecosystems, ranging from 242 to 374 mm/yr in grasslands, 213 to 278 mm/yr in boreal forests, and 100 to 199 mm/yr in semi-desert and desert regions. The rate of ET increase follows the order of grasslands, semi-deserts/deserts, and boreal forests, reflecting underlying ecological and climatic gradients. While climate-induced land cover changes (LCCs) are evident, their effect on ET has been relatively minor, with a difference of less than 5% compared to a static land cover baseline. This indicates that climate change, rather than LCC alone, is the dominant driver of ET variability across the plateau [18].

1.2 Objective of the study

Mongolian plateau's geographic position and geomorphological diversity further intensify its vulnerability to climate fluctuations, especially in the ecotone between desert and steppe ecosystems [19]. The regional economy depends mainly on extensive livestock grazing, which requires vast areas of pastureland. These grassland resources, however, are susceptible to both temperature and precipitation conditions, which directly influence pasture productivity and, consequently, local communities' livelihoods and economic security.[20] Understanding the interplay between vegetation dynamics and climate change across the Mongolian Plateau is therefore vital for ecological

Given these vulnerabilities, understanding the interaction between vegetation dynamics and climate change across the Mongolian Plateau is essential for guiding ecological management and policy-making. This study, by integrating long-term satellite observations of vegetation (NDVI), temperature (LST), and ET, offers a scientific foundation for evidence-based decision-making. Classifying vegetation–climate response types and identifying spatial patterns in environmental stress can inform regional climate adaptation strategies, targeted rangeland restoration, and land-use planning.

Ultimately, this research contributes to a deeper understanding of ecosystem sensitivity in semi-arid regions and can be used as a baseline study for long-term monitoring, environmental planning, and climate adaptation in some areas of the Mongolian Plateau.

2. Methodology

2.1 Study Area

For this research, three representative mining-influenced sub-regions were selected to capture the diversity of environmental conditions across the plateau.

The first region, comprising 18 soums and an area of approximately 229,028.27 km², represents the transboundary desert region between southern Mongolia and Inner Mongolia, characterized by an arid desert climate. Precipitation is extremely low, typically ranging from 50 to 150 mm per year, while surface evaporation exceeds 800–1000 mm annually, resulting in a persistent moisture deficit. The annual mean temperature is approximately 6°C, with January averages ranging from –15 °C to –12°C, and summer temperatures (in July) reaching 25°C. NDVI values in this zone are very low (0.05–0.18), reflecting minimal vegetation cover. Wind speeds are relatively high, typically ranging from 4 to 6 meters per second, contributing to dust storms and surface erosion.[4]

Table 1. Soums of the transboundary desert region between southern Mongolia and Inner Mongolia, and the corresponding area

Mongolia		Inner Mongolian Autonomous Region (China)			
Umnugobi province		Alxa league		Bayannuur city	
Soum name	Area, km2	Soum name	Area, km2	Soum name	Area, km2
Bayan	11168.319	Bayan Toroi	4237.919	Ganqimaodu	4336.834
Bayandalai	10656.452	Ceke	236.378	Urad Rear Banner	24323.24
Hurmen	12655.925	Dongfeng	11132.337		
Khanbogd	14963.112	Inggen	6789.097		
Nomgon	18460.41	Olji	7580.723		
Noyon	10561.251	Ontuul	15710.71		
		Saihan Toroi	21676.85		
		Suvnuur	4623.142		
		Tansagbulag	21949.825		
Sum	78465.469		93936.981		cc

The soums' areas are calculated and extracted from QGIS.

The second region comprises 16 soums and spans approximately 143,049.19 km² across the steppe zone of Eastern Mongolia and Inner Mongolia, where both climate variability and human land-use pressure drive significant ecological changes. This area experiences moderate precipitation levels, typically 150 to 250 mm per year, with an annual average temperature of around 2°C. Winters are harsh, with January temperatures dropping to –20 to –25°C, while summers are milder, with July temperatures ranging from 20 to 25°C, particularly in the Dornod

steppe. Surface evaporation rates are moderately high (650–750 mm/year), and NDVI values range from 0.2 to 0.35, indicating seasonal vegetation activity. Like the desert zone, wind speeds range from 4 to 6 m/s, especially across the open plains.[4]

Table 2. Souns of the transboundary steppe region between eastern Mongolia and Inner Mongolia, and the corresponding area

Mongolia		Inner Mongolian Autonomous Region (China)			
Dornod province		Xiliin Gol league		Hulunbuir city	
Soum name	Area, km ²	Soum name	Area, km ²	Soum name	Area, km ²
Chuluunkhoroot	6406.557	Bogd	720.85	New Barag Left Banner	19917.63
Gurvanzagal	5257.084	Gahail	5251.926	New Barag Right Banner	25131.421
Choibalsan	10125.841	Mandahbulag	4741.109		
Bayantumen	8393.193	Samai	5964.922		
Herlen	284.706				
Matad	22825.686				
Halhgoi	28028.265				
Sum	81321.332		16678.807		45049.051

The third focus area is located in northern Mongolia, encompassing 21 soums with a total area of 44,589.55 km² across the Darkhan-Uul and Selenge provinces. This region lies within Mongolia's forest-steppe and agricultural belt, representing one of the country's most ecologically productive and densely vegetated areas.

It features more favorable climatic and hydrological conditions, with precipitation ranging between 250–300 mm per year and lower surface evaporation rates (550–700 mm/year). Due to the valley-dominated topography, the annual mean temperature ranges from –6 to –8°C, with extreme winter temperatures reaching –30 to –34°C in January. July temperatures are moderate, between 15–20°C across the Orkhon, Selenge, and Khalkh river basins. The NDVI values are highest in this zone (0.4–0.5), particularly in forested areas, reflecting dense and productive vegetation cover. Wind conditions are milder, with speeds ranging from 2 to 3 m/s. [4] This region is ecologically rich and agriculturally significant, supported by major river systems such as the Selenge, Orkhon, Kharaa, Tuul, and Yeruu, which contribute to localized climatic

variation due to terrain complexity and surface heterogeneity.[21] These differences in topography, land cover, and solar energy absorption further influence microclimatic conditions, making this region a key focus for studying the interactions between vegetation, climate, and human activity. [22]

Table 3. Soums of northern Mongolia (Selenge and Darkhan provinces), and the corresponding area

Mongolia					
Selenge province				Darkhan province	
Soum name	Area, km ²	Soum name	Area, km ²	Soum name	Area, km ²
Altanbulag	2441.542	Sant	1354.759	Darkhan	100.923
Baruunburen	2810.615	Shaamar	619.221	Orkhon	463.338
Bayangol	1995.37	Sukhbaatar	47.011	Khongor	2531.068
Javkhlant	1189.599	Tsagaannuur	3803.154	Shariin Gol	95.425
Khuder	2648.153	Tushig	2523.316		
Khushaat	2008.892	Yeroo	8370.245		
Orkhon	1317.988	Zuunburen	1195.446		
Orkhontuul	2920.011	Zuunkharaa	4845.003		
Saikhan	1308.47				
Sum	41398.795				3190.754

These regions were chosen not only for their ecological importance but also due to the availability of long-term satellite and climate data, administrative clarity (based on soums and town boundaries), and their strategic relevance for future land management and climate adaptation planning.

2.2 Satellite data sources and processing

This study used satellite-derived raster datasets from NASA's MODIS sensor onboard the Terra satellite to monitor vegetation activity, land surface temperature, and evapotranspiration across the Mongolian Plateau. The datasets were accessed and downloaded via the Google Earth Engine (GEE) platform using the JavaScript Application Programming Interface (API).

Specifically, the **Normalized Difference Vegetation Index (NDVI)** was obtained from the MODIS product MOD13A2 v6.1, which provides 16-day composites at a spatial resolution of 1 km. At the same time, **Land Surface Temperature (LST)** was retrieved from MOD11A1 v6.1, offering daily daytime surface temperature data at 1 km resolution. Both datasets were filtered to extract monthly mean values for the growing season months (May to August) for each year from 2000 to 2024, resulting in a rich archive of 25 years of vegetation and thermal data over the entire Mongolian Plateau.

The downloaded raster data were processed using QGIS 3.34.9. Within QGIS, the cell statistics processing tool was used to compute annual summer averages (May–August) for each year and to generate long-term (2000–2024) composite maps. This spatial-temporal averaging enabled the visualization of broad patterns in vegetation dynamics (via NDVI) and surface temperature changes (via LST) across the region. The resulting maps, with a spatial resolution of 1 km, clearly highlight geographic differences and long-term trends in land surface characteristics.

Evapotranspiration (ET) was estimated using a method adapted to Mongolian conditions by Dr. Tuya S, based on the classical **Bowen Ratio Energy Balance (BREB) method** initially proposed by physicist Ira Sprague Bowen in 1926. This method utilizes satellite-derived surface temperature and vegetation indices to estimate spatially distributed latent heat flux (LE), which is then converted to actual ET. [14]

The fundamental energy balance equation used is:

$$LE = (Rn - G) - H$$

Where:

- LE is the latent heat flux (MJ/m²/day),
- Rn is the net radiation (MJ/m²/day),
- G is the ground heat flux (MJ/m²/day),
- H is the sensible heat flux (MJ/m²/day).

By expressing the Bowen ratio $\beta = \frac{H}{LE}$, the equation can be rearranged as:

$$LE = \frac{Rn - G}{1 + \beta}$$

To estimate the Bowen ratio β , Tuya's model uses empirical relationships that link MODIS-derived NDVI and LST to surface energy partitioning. Specifically, latent heat is expressed as a function of NDVI and LST as follows:

$$LE = f_1(NDVI) \times f_2(LST)$$

Where f_1 and f_2 are functions derived from NDVI and LST, respectively. The resulting latent heat flux is then converted to evapotranspiration using:

$$ET = 0.408 \times LE$$

$$ET = [0.56 \times \ln(NDVI) + 1.8] \cdot (0.467 \times LST - 14)$$

Where:

- ET is the daily evapotranspiration rate (mm/day),
- $NDVI$ is the Normalized Difference Vegetation Index,
- LST is the daytime Land Surface Temperature in °C.

This formulation considers surface energy balance, vegetation cover, and land surface temperature, making it well-suited for Mongolia's highly variable steppe and desert environments. The final output is expressed in mm/day, assuming a conversion of 1 MJ/m²/day \approx 0.408 mm/day, based on FAO (1998) guidelines, where 1 kg of water requires 2.45 MJ to evaporate.

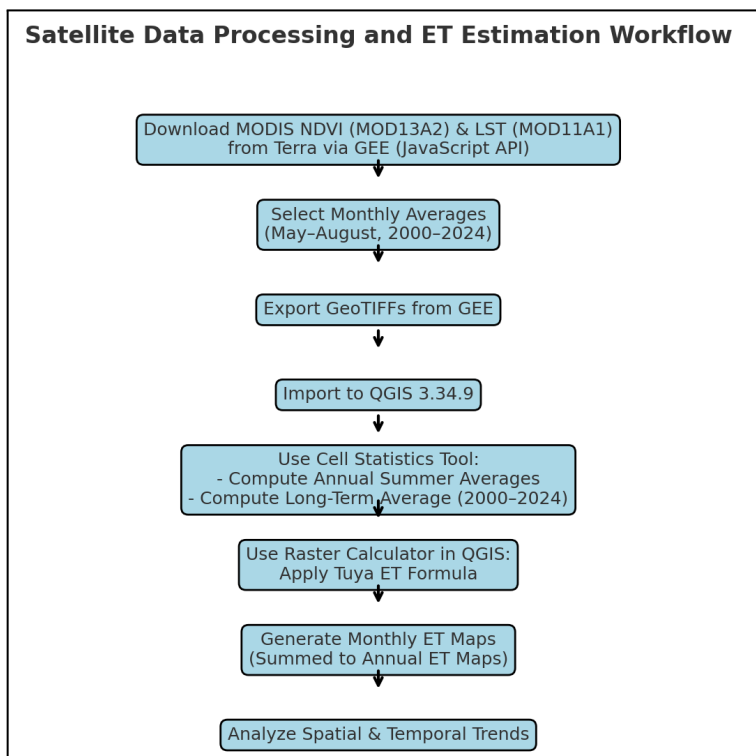


Figure 1. Satellite data processing and ET estimation workflow

This computation was performed using the Raster Calculator tool in QGIS. Monthly ET maps were generated for each summer month, and then summed to produce annual summer ET maps for each year in the 2000–2024 period. These ET rasters provide a spatially explicit record of evapotranspiration behavior across the Mongolian Plateau, allowing for comparative

analysis across years and ecological zones.

2.3 Estimation of standardization and normalization

To evaluate climate and vegetation variability across the Mongolian Plateau from 2000 to 2024, this study applied **normalization** and **standardization** to annual raster datasets for NDVI, LST, and ET. These processes enabled consistent scaling and detection of environmental anomalies across space and time.

2.3.1 Normalization Process

Annual raster layers for each parameter were first normalized using the min-max normalization method. This step scaled each pixel value to a range between 0 and 1, allowing for direct comparison across parameters with different units and ranges. Importantly, due to differences in interpretation, two normalization strategies were applied. (Table 4)

Table 4. Normalization equation for each parameter

Parameter	Equation
Land surface temperature and Evapotranspiration	$X_{norm} = \frac{X_i - X_{min(i)}}{X_{max(i)} - X_{min(i)}}$
Normalized Vegetation Difference Index	$X_{norm} = \frac{X_{max(i)} - X_{(i)}}{X_{max(i)} - X_{min(i)}}$

This ensured that in all cases, lower normalized values represented more stressed conditions, and higher values represented more favorable ones. The normalization was applied using the Raster Calculator tool in QGIS and resulted in annual normalized raster products from 2000 to 2024 at 1 km resolution.

2.3.2 Standardization Process

Following normalization, standardization was applied to quantify the degree of deviation from multi-year norms using the Z-score method. For each normalized raster series (NDVI, LST, ET), the mean and standard deviation were calculated from the 25-year period (2000–2024). Standardization was performed using the formula in Table 5.

Table 5. Standardization equation for each parameter

Parameter	Equation
Land surface temperature, Evapotranspiration, and Evapotranspiration	$X_{standard} = \frac{X_i - X_{mean(2000-2024)}}{\sigma_{(2000-2024)}}$

This process generated standardized anomaly maps, indicating the number of standard deviations by which each year's value deviated from the long-term mean. The standardized rasters were produced using QGIS Raster Calculator for each year.

2.3.3 Thresholding and Conditioned Maps

To focus on significant deviations, the standardized rasters were conditioned using thresholds. Pixels with Z-scores between -0.5 and $+0.5$ were considered stable and excluded from anomaly detection, while those with Z-scores outside this range were interpreted as either stressed or improving.

To unify the interpretation of standardized Z-score rasters across different parameters, a conditioning transformation was applied. Since standardized values can be both positive and negative, a direct comparison between variables such as NDVI, LST, and ET can be inconsistent. For example, negative Z-scores in NDVI indicate vegetation loss, while positive Z-scores in LST and ET indicate environmental stress. To standardize the scale and direction of interpretation, NDVI Z-scores below -0.5 were multiplied by -1 , converting negative deviations into positive stress values. Meanwhile, LST and ET values above $+0.5$ were retained as-is. This transformation ensured that all output values were positive and that higher values consistently indicated more severe environmental stress or degradation, while zero or near-zero values indicated stable conditions.

Table 6. Thresholding conditions for standardized values

Parameter	Equation
Land surface temperature and Evapotranspiration	$(X_{standard} > 0.5) * X_{standard}$
Normalized Vegetation Difference Index	$(X_{standard} < -0.5) * - X_{standard}$

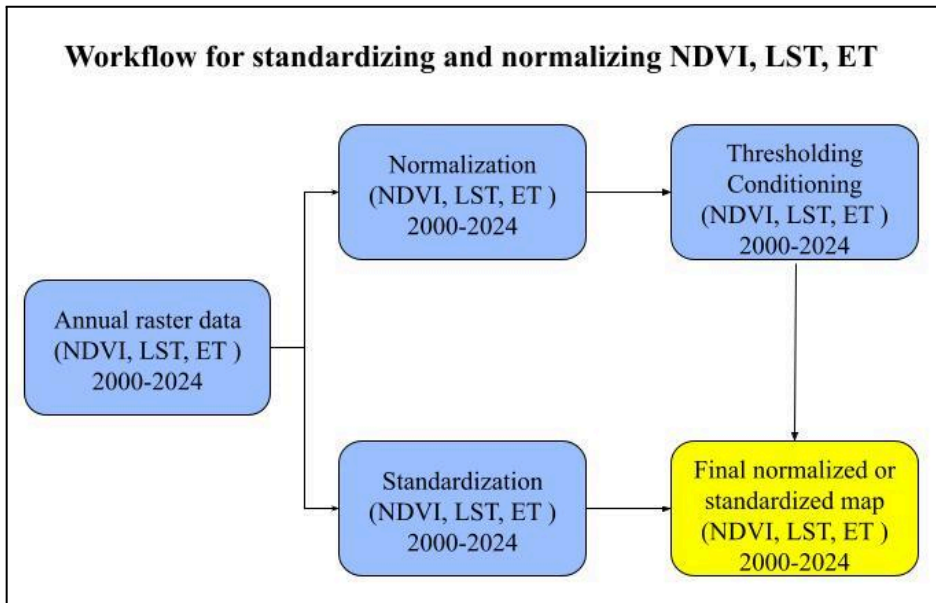


Figure 2. Workflow for standardizing and normalizing NDVI, LST, ET

2.4 Weight Determination Using Analytic Hierarchy Process (AHP)

To integrate the three environmental indicators (NDVI, LST, ET) into a composite standardized and normalized index, weights were assigned to each parameter using the Analytic Hierarchy Process (AHP). The AHP, introduced by Thomas L. Saaty, is a well-established multi-criteria decision-making method that derives the relative importance of decision factors through structured pairwise comparisons. [23, 25] This method is particularly suitable for environmental studies that require synthesizing complex, multidimensional datasets using expert-informed reasoning.

A pairwise comparison matrix was constructed to derive the weights, in which each criterion was compared with every other criterion based on its relative importance in relation to the overall goal. The comparisons were made using Saaty's fundamental 1–9 scale (Table 7), where 1 indicates equal importance and 9 indicates extreme importance of one criterion over another. Reciprocals (e.g., 1/3, 1/5) were used for inverse comparisons.[23] The resulting comparison matrix is a square reciprocal matrix with diagonal values are 1 (indicating self-comparison).

Table 7. Saaty's fundamental scale

Score	Definition	Explanation
1	Equal importance	2 activities contribute equally to the objective
3	Moderate importance	Experience and judgement strongly favour one activity over another

5	Strong importance	Experience and judgement strongly favour one activity over another
7	Very strong importance	An activity is strongly favoured and its dominance is demonstrated in practice
2, 4, 6, 8	Intermediate values	When compromise is needed
9	Extreme importance	The evidence favouring one activity over another is of the highest possible order of affirmation
1/3, 1/5, 1/7, 1/9	Values for inverse comparison	

Once the matrix was constructed, the priority (weight) vector was derived. This involves computing the geometric mean of each row in the matrix and then normalizing the resulting vector so that all weights sum to 1. Alternatively, the principal eigenvector corresponding to the matrix's largest eigenvalue λ_{max} can be used. [24] This study employed the geometric mean method due to its computational simplicity and comparability with eigenvalue-based results, particularly in three-dimensional matrices. These weights reflect the relative importance of each criterion in assessing environmental stress.

To ensure that the pairwise judgments were logically consistent, the Consistency Index (CI) and Consistency Ratio (CR) were calculated. The CI was obtained using the formula $CI = (\lambda_{max} - n)/(n - 1)$, where n is the number of criteria. This value was then compared against the Random Index (RI) (Table 9), which represents the average consistency index for randomly generated matrices of the same size. [25]

Table 8. The value of the random consistency index

Attributes	3	4	5	6	7	8	9	10
Random index	0.52	0.89	1.11	1.25	1.35	1.4	1.45	1.49

The consistency ratio is calculated as $CR = RI/CI$. A CR value less than 0.1 indicates acceptable consistency, meaning that the judgments made in the matrix are reliable enough to be used in further analysis. [23, 25]

If the CR is below this threshold, the derived weights can be considered logically sound and suitable for integration into further analysis. After validating the consistency, the final weights were used to combine the normalized and standardized raster layers of NDVI, LST, and ET. Using the QGIS raster calculator, two composite maps were generated. (composite normalized map and a composite standardized map) Each map is created by summing the products of the AHP-derived weights and the respective parameter layers. This operation ensured that each

variable contributed proportionally to the final index according to its influence on environmental stress.

Table 9 in the thesis summarizes the AHP variables used and their respective formulas. It outlines the steps for calculating the maximum eigenvalue, consistency index, and consistency ratio, reinforcing the transparency and reproducibility of the methodology. These steps ensure that the derived weights are not only mathematically sound but also logically justifiable.

Table 9. Variables and formulas used in AHP weight calculation

#	Variable	Description
1	M matrix	Pairwise comparison matrix constructed between criteria
2	Fundamental scale	Saaty's scale is used to assign scores in the pairwise matrix (Table 7)
3	RI (Random Index)	Random index used in the consistency check, depends on the number of criteria (Table 8)
4	λ_{max}	Maximum eigenvalue of the pairwise matrix M
5	CI (Consistency Index)	$CI = (\lambda_{max} - n)/(n - 1)$; Measures the consistency of judgments
6	CR (Consistency Ratio)	$CR = RI/CI$ If $CR < 0.10$, the matrix is considered consistent

2.5 Classification of vegetation-climate response type analysis

To better understand the relationship between vegetation performance and climatic stress, each soum across the Mongolian Plateau was classified into one of four Vegetation–Climate Response Types (VCRT) based on its environmental conditions and interannual variability. This classification was based on a scatter plot built using an R script executed in RStudio, an open-source programming language and software environment used mainly for statistical computing and graphics.

Each point on the plot represents a soum, plotted according to its composite normalized index (x-axis), which reflects long-term average environmental conditions, and its composite standardized index (y-axis), which reflects interannual variability or ecological changes. The normalized index captures the overall environmental quality (NDVI vs. LST and ET), while the standardized index reveals interannual variability. The scatter plot was divided into four quadrants using red dashed lines representing each index's mean values, thus forming a two-dimensional matrix for classification.

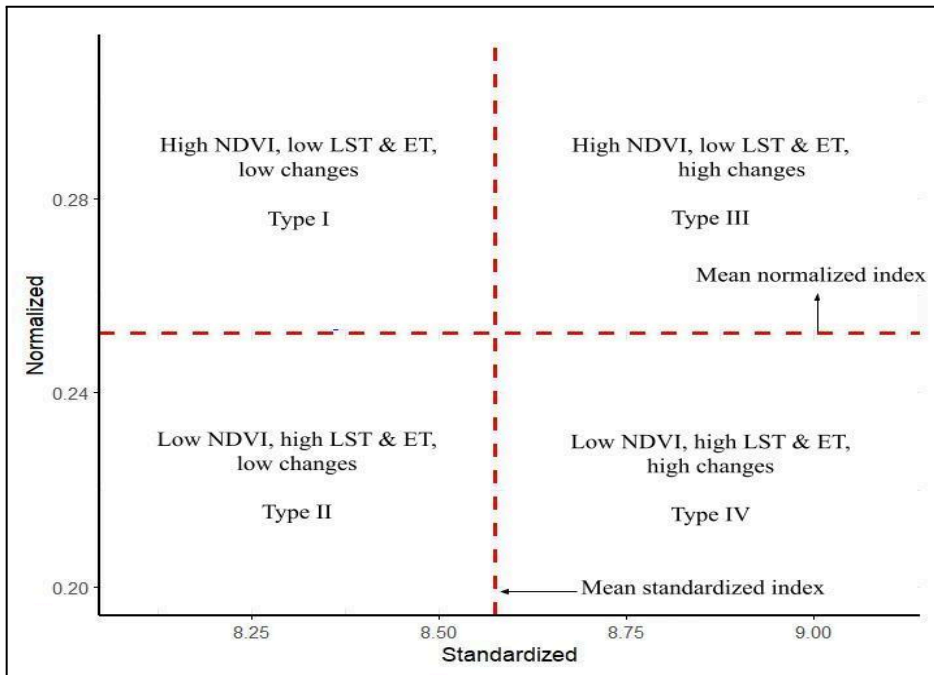


Figure 3. Classification of Vegetation–Climate Response Types based on Normalized and Standardized Composite Indices

This classification yielded four response types:

Type I – *High NDVI, Low LST and ET, Low Interannual Variability*: These areas exhibit favorable long-term vegetation conditions and stable climate, indicating resilient ecosystems with minimal stress.

Type II – *Low NDVI, High LST and ET, Low Interannual Variability*: These areas experience long-term climatic stress, characterized by high heat and evapotranspiration, resulting in low vegetation productivity, but with stable patterns over time.

Type III – *High NDVI, Low LST and ET, High Interannual Variability*: These zones exhibit strong vegetation performance under favorable climatic conditions, but with high year-to-year fluctuations. These points are located in the upper-right quadrant, indicating sensitivity to climate extremes or land-use shifts.

Type IV – *Low NDVI, High LST and ET, High Interannual Variability*: These represent ecologically vulnerable areas characterized by degraded vegetation, harsh climate conditions, and significant year-to-year fluctuations.

After classification, the mean standardized and normalized composite indices were extracted for each soum to quantify their relative position within the four response types. Using these values, each soum was assigned a corresponding vegetation–climate response type based on its quadrant in the scatter plot. The data were grouped accordingly and exported for spatial visualization.

The grouped response types were joined with geographic boundary shapefiles in QGIS to generate a spatial representation of the classification results. A final classified map was produced, showing the distribution of the four vegetation–climate response types across the three study areas.

3. Results and Discussion

3.1 NDVI and LST mapping from 2000 to 2024

In this part, 200 individual raster datasets of NDVI and LST from May to August, 2000–2024 were compiled and averaged annually, resulting in 25 composite rasters for each parameter. As a visual example of these inputs, the mean NDVI and LST for July 2000 and the seasonal average (May–August 2000) are shown in Figure 4 to 7.

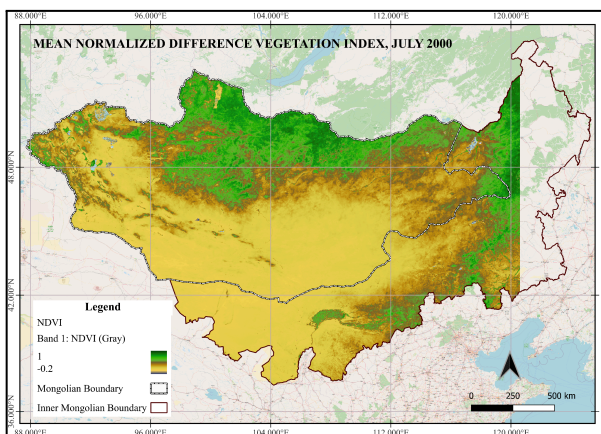


Figure 4. Mean NDVI of July 2000

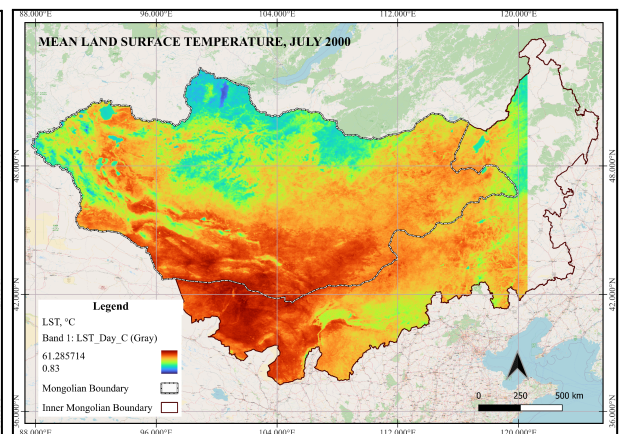


Figure 5. Mean LST of July 2000

/Clear maps shown in the appendix/

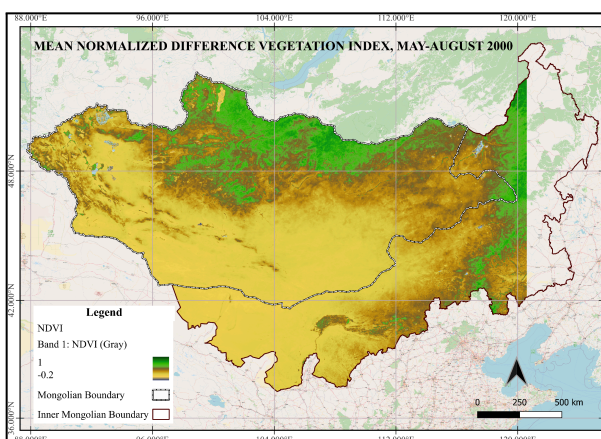


Figure 6. Mean NDVI of May to August 2000

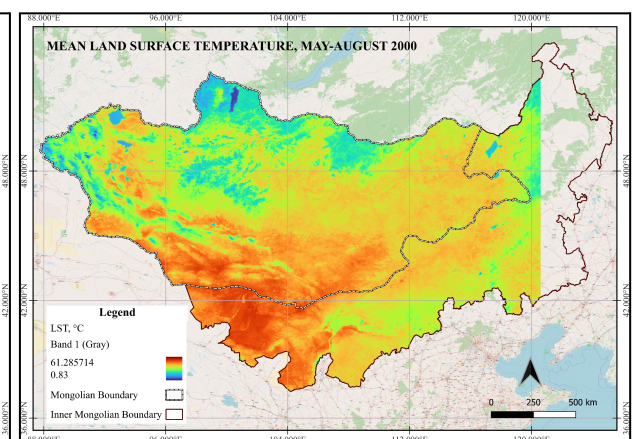


Figure 7. Mean LST of May to August 2000

The LST maps for May to August (Figure 7) and July 2000 (Figure 5) reveal a clear north–south thermal gradient. The southern Gobi Desert and adjacent parts of Inner Mongolia exhibit high surface temperatures, often exceeding 40°C, reflecting arid conditions with intense solar radiation and sparse vegetation. In contrast, northern and mountainous regions show much cooler temperatures, often below 25°C, influenced by elevation, forest cover, and greater evapotranspiration buffering.

The July LST map, representing the peak heat period, highlights intensified surface temperatures compared to the seasonal average, with widespread thermal maxima observed in steppe and desert zones.

NDVI maps for July (Figure 4) and May–August (Figure 6) similarly exhibit a strong north–south gradient in vegetation density and productivity. High NDVI values (>0.5) dominate the northern forest steppe and river valley zones, indicating lush, actively photosynthesizing vegetation during the peak growing season. By contrast, the southern arid regions, especially the Gobi and Alxa Plateau, show very low or negative NDVI values, reflecting barren or sparsely vegetated surfaces.

The seasonal NDVI average (May–August) provides a more stable depiction of regional vegetation dynamics, capturing the cumulative response of ecosystems across the growing season and filtering short-term variability.

3.2 Estimation of ET using NDVI and LST

Following the approach proposed by Dr. Tuya S. for estimating land surface evapotranspiration (ET) in Mongolia using the MODIS sensor's NDVI and LST raster data, summer-time (May to August) ET raster values were calculated for the selected study area for each year from 2000 to 2024. This method utilizes the strong correlation between vegetation activity and surface temperature to derive spatially distributed evaporation estimates.

As an example of the model results, the average results for July 2000 and the cumulative data for May to August of that year are shown in Figures 8,9. / *Clear maps shown in the appendix/*

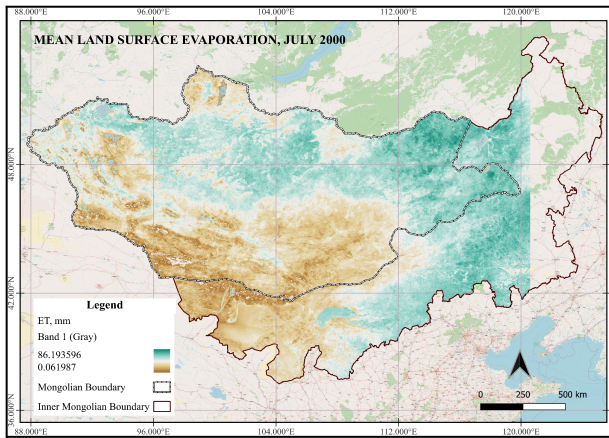


Figure 8. Mean ET of July 2000 and

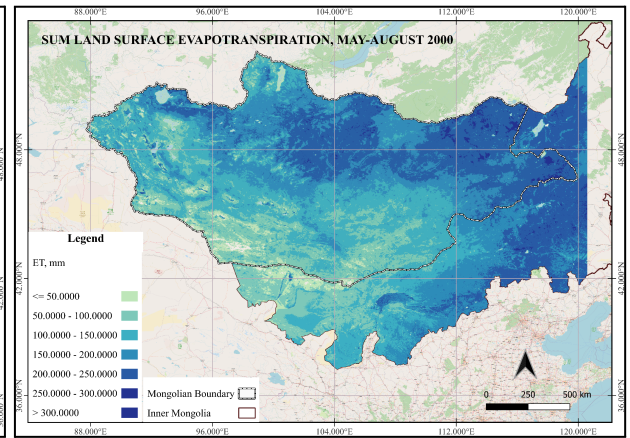


Figure 9. Sum ET of May to August 2000

From Figure 9. In the southern flat terrains of the Khangai region, particularly in low-lying lake basins and desert-steppe zones dominated by feather grass (*Stipa spp.*) and wormwood (*Artemisia spp.*), actual annual precipitation values range between 50–150 mm.

In contrast, regions such as eastern Khangai, southern Khentii, and the lowland floodplains of the Orkhon and Tuul rivers, characterized by relatively lower elevation but favorable geomorphological settings, exhibit precipitation levels exceeding 250 mm/year.

Moreover, areas encompassing the Mönkh Khan Ridge, the hazaar grass-steppe, and the sharilj–feather grass transition zones record annual precipitation values between 150–250 mm. These observed values align well with modeled precipitation estimates, indicating a high degree of correlation between simulated outputs and ground-based climatic data. This correspondence reinforces the reliability of spatial precipitation models in reflecting actual hydrometeorological conditions across the Mongolian Plateau.

3.3 Calculation of the normalized climate and vegetation Index

The normalized climate and vegetation index, also known as the summer condition (zunshlaga), was used to evaluate the combined climate and vegetation conditions of the study area. To calculate this index, the minimum and maximum values of each parameter were extracted directly from the raster data for each year from 2000 to 2024. These extracted values are summarized in Table 10.

Table 10. Minimum and maximum values of each parameter by the Mongolian Plateau

Parameter	ET, mm		LST, °C		NDVI	
	Max	Min	Max	Min	Max	Min
Year						

2000	290.341	0.014	54.090	2.744	0.836	-0.158
2001	287.569	0.011	53.178	3.430	0.820	-0.174
2002	286.864	0.018	53.414	3.936	0.847	-0.136
2003	263.697	0.053	51.510	2.279	0.857	-0.150
2004	272.911	0.062	52.236	3.809	0.831	-0.140
2005	264.680	0.015	54.244	2.003	0.826	-0.125
2006	254.401	0.010	53.611	1.315	0.818	-0.170
2007	278.051	0.012	53.354	3.542	0.827	-0.142
2008	270.604	0.014	52.284	3.751	0.832	-0.157
2009	258.906	0.012	53.234	2.622	0.844	-0.161
2010	275.546	0.054	51.965	2.632	0.838	-0.168
2011	257.431	0.049	53.024	2.996	0.822	-0.154
2012	253.929	0.071	53.753	3.876	0.864	-0.167
2013	247.603	0.045	53.564	1.542	0.835	-0.166
2014	253.851	0.014	52.530	2.383	0.866	-0.135
2015	273.055	0.106	52.673	4.228	0.849	-0.117
2016	270.557	0.057	53.532	2.519	0.860	-0.143
2017	274.933	0.014	54.591	5.100	0.873	-0.137
2018	263.989	0.012	53.758	3.650	0.879	-0.163
2019	271.259	0.010	52.255	3.156	0.866	-0.128
2020	260.620	0.015	53.366	2.691	0.856	-0.122
2021	255.570	0.015	53.421	3.347	0.849	-0.134
2022	257.209	0.013	53.495	4.524	0.870	-0.124
2023	256.796	0.014	52.226	2.008	0.865	-0.140
2024	257.661	0.013	51.668	4.848	0.840	-0.145

Annual normalization was then performed using the Raster Calculator tool in QGIS, applying the standard normalization formula presented in Table 4.

After producing the annual normalized raster images, the long-term average normalized rasters for the period 2000–2024 were created by calculating the mean of the yearly normalized results for each parameter. The resulting long-term average normalized maps for NDVI, LST, and ET

are presented in Figures 10-12, illustrating the overall spatial distribution of climate and vegetation conditions across the study area over the 25 years.

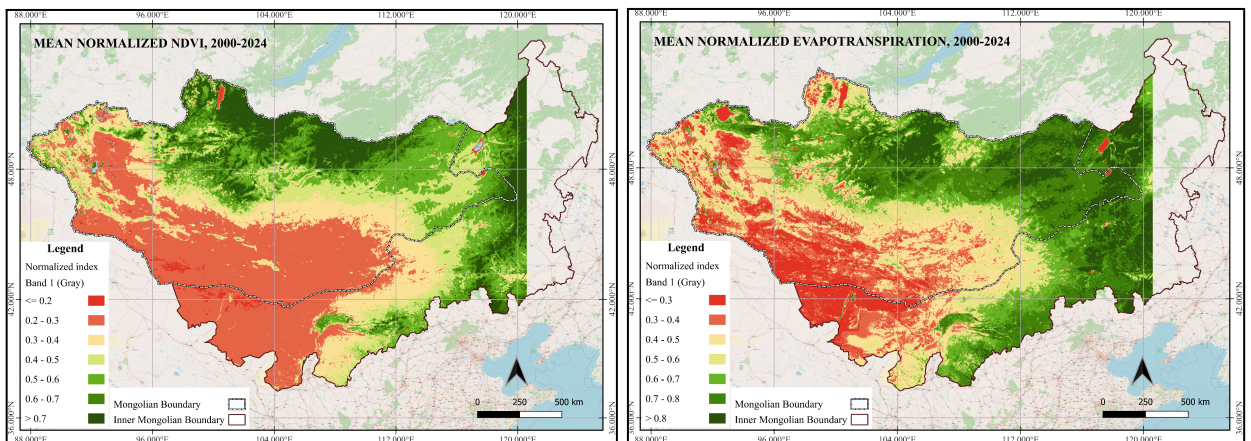


Figure 10. Mean normalized NDVI of 2000-2024 Figure 11. Mean normalized ET of 2000-2024

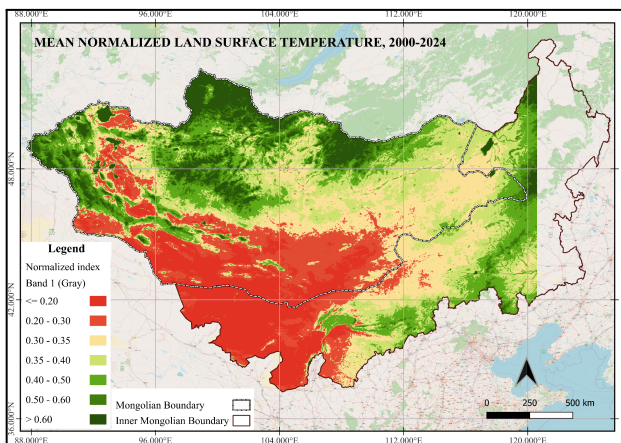


Figure 12. Mean normalized LST of 2000-2024 / Clear maps shown in the appendix/

As previously mentioned, the normalized index reflects the summer-time climate and vegetation conditions (zunshлага) of the selected study area. Analysis of Figure 10-12 indicates that the southern region experiences poorer summer conditions, as evidenced by elevated LST, lower NDVI values, and reduced ET rates. Conversely, the northern region demonstrates more favorable summer conditions, with lower LST, ET, and higher NDVI values. The eastern region generally exhibits average conditions, whereas the western region shows a heterogeneous pattern, with some areas performing above average and others below average.

These spatial variations highlight the significant impact of inherent geophysical and geomorphological characteristics on summer-time conditions. Therefore, direct comparisons between areas with differing natural attributes may lead to misleading interpretations. To ensure robust and reliable analyses, it is thus necessary to evaluate and compare regions with similar geophysical and geomorphological features.

3.4 Calculation of the standardized climate and vegetation index

To assess climate and vegetation changes, annual standardized raster products were produced by calculating the yearly deviation (Z-score) values for NDVI, LST, and ET, which were generated each year from 2000 to 2024. Standardization was performed based on the interannual mean and standard deviation values calculated from the 2000–2024 dataset. Annual standardization was then performed using the Raster Calculator tool in QGIS, applying the standardization formula presented in Tables 5 and 6.

Following standardization, yearly raster maps for NDVI, LST, and ET were summed across all years to quantify the cumulative deviation of each parameter throughout the study period. The resulting composite deviation maps reveal spatial patterns of long-term anomalies, allowing for the identification of areas experiencing persistent ecological or climatic shifts.

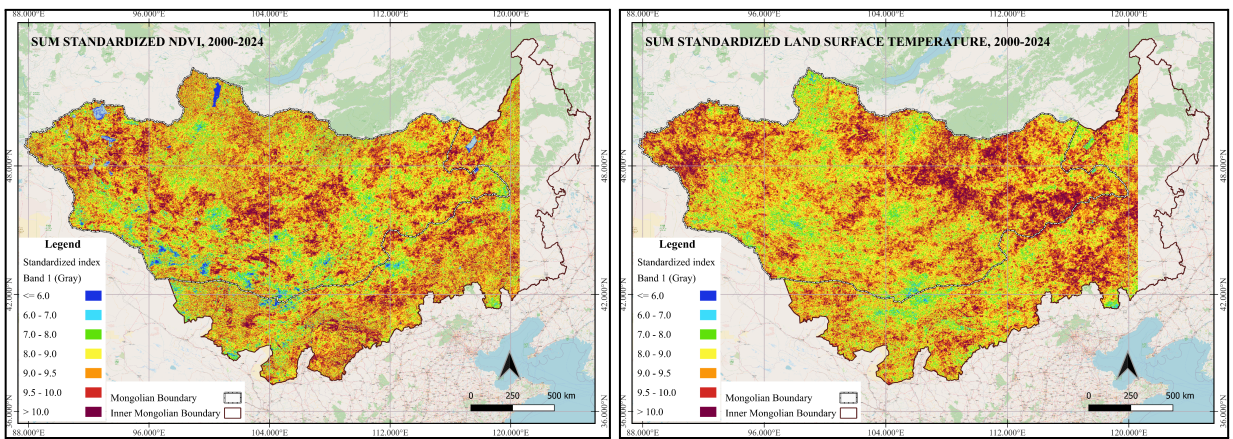


Figure 13. Sum standardized NDVI (2000-2024) Figure 14. Sum standardized LST(2000-2024)

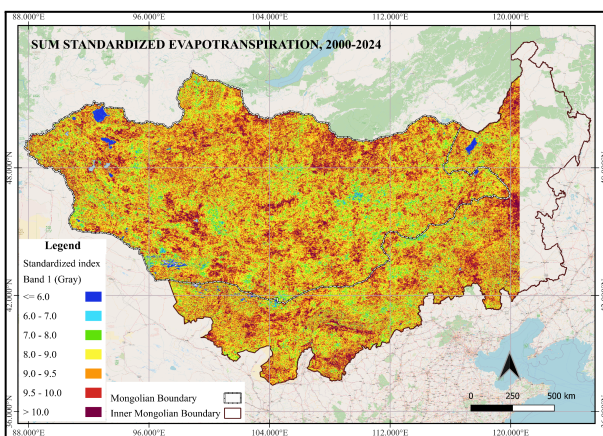


Figure 15. Sum standardized ET (2000-2024) / Clear maps shown in the appendix/

Figures 13 to 15 present the cumulative standardized deviation maps of NDVI, LST, and ET from 2000 to 2024 across the Mongolian Plateau. These maps visualize the long-term deviation

of each variable from its interannual mean, highlighting spatial heterogeneity in environmental conditions.

The summed NDVI Z-score map (Figure 13) reveals pronounced negative deviations (red to dark red) across central and southeastern regions, indicating persistent vegetation stress or degradation over the 25 years. In contrast, certain areas in the northern and northwestern regions exhibit positive deviations (blue to green), indicating relatively stable or improved vegetation conditions.

The LST deviation map (Figure 14) shows extensive regions with high negative values, particularly in the central and southern areas, indicating sustained increases in land surface temperature. These warming trends are likely to contribute to vegetation stress and increased evapotranspirative demand.

Similarly, the ET deviation map (Figure 15) exhibits a comparable spatial pattern to LST, with high cumulative Z-scores in the southern and southeastern parts. This may reflect increased evaporative loss and associated moisture stress in arid and semi-arid zones, further exacerbating ecological vulnerability.

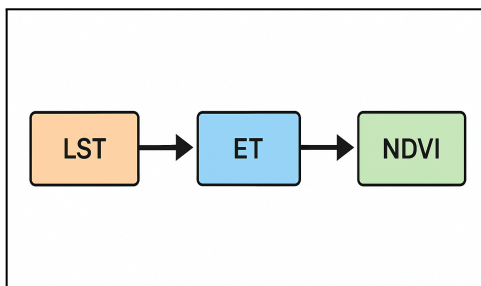
Collectively, these standardized maps highlight apparent shifts in climatic and vegetation patterns over the study period, providing the basis for subsequent integration using weighted overlay and classification into Vegetation–Climate Response Types.

3.5 Weighted integration of parameters using Pair-Wise Comparison method

To integrate NDVI, LST, and ET into a single composite index that reflects climate–vegetation interactions, the Analytic Hierarchy Process (AHP) was applied through a pair-wise comparison matrix to determine the relative importance (weight) of each parameter. Three different pair-wise comparison matrices were developed to explore weighting sensitivity and ensure consistency in judgment. The matrix with the **lowest Consistency Index (CI)** was selected for final weighting, ensuring logical coherence in the assigned values.

3.5.1 Parameter Relationship and Conceptual Ordering

The order of parameters in the pair-wise comparison matrix was not arbitrary, but rather grounded in their ecological interactions. LST was treated as the anchor parameter,



representing the primary climatic driver influencing surface energy balance. ET was considered a follower parameter, dynamically responding to variations in temperature and atmospheric demand. Finally, NDVI was positioned as the resulting parameter, reflecting the cumulative impact of thermal and moisture conditions on vegetation productivity.

Figure 16. The order of the parameters

This conceptual hierarchy aligns with the understanding that climatic conditions both directly and indirectly influence vegetation health. By placing NDVI as the outcome variable and LST as the dominant forcing factor, the selected weighting scheme better captures the causal relationship between climate and vegetation responses across the Mongolian Plateau.

3.5.2 Development and Evaluation of Comparison Matrices

Three pair-wise comparison matrices were constructed with slightly different input values to test the consistency index. Each matrix was assessed for internal consistency using the **Consistency Index (CI)** and **Consistency Ratio (CR)**, derived from the principal eigenvalue.

The comparison of matrix performance is shown in Table 11.

Table 11. Summary of Consistency Metrics for Three Matrices

Matrix ID	Eigenvalue(λ)	Consistency Index (CI)	Consistency Ratio (CR)	Status
Matrix 1	3.007	0.004	0.007	Selected
Matrix 2	3.054	0.027	0.052	Acceptable
Matrix 3	3.086	0.043	0.082	Acceptable

Matrix 1 was selected due to its lowest CR value ($0.007 < 0.10$), ensuring high consistency in the relative judgments.

Table 12. Chosen Pair-Wise Comparison Matrix

	M1			Geometric average	M2	M3	M4=M3/M2
	LST	ET	NDVI		weight		
LST	1	0.333	0.143	0.362	0.0879	0.264	3.007
ET	3	1	0.333	1.000	0.2426	0.730	3.007
NDVI	7	3	1	2.759	0.6694	2.013	3.007
				4.121	1.000	$\lambda_{max}=\sum M4i/n$	3.007
						consistency index	0.004
						random index (n=3)	0.52
						consistency ratio	0.007
						consistant	$0.007 < 0.10$

The principal eigenvalue was calculated as $\lambda_{max}=\sum M4i/n= 3.007$, and the **consistency Index (CI)** was computed as **0.004**. With a random Index (RI) of 0.52 for $n = 3$ (Table 8), the resulting **consistency Ratio (CR)** was **0.007**, confirming a high level of consistency ($CR < 0.10$) in the judgments made.

Using the final weights of NDVI (0.669), ET (0.243), and LST (0.088), two types of composite maps were produced to represent integrated climate–vegetation dynamics. The first, a standardized weighted map (Figure 17), was created by multiplying each standardized Z-score raster (NDVI, LST, ET) by its corresponding weight and summing the results using the Raster Calculator in QGIS. The second, a normalized weighted map (Figure 18), was generated by applying min–max normalization (scaling each parameter to a 0–1 range), then weighting and

summing the layers. These two approaches offer complementary perspectives: the standardized map highlights deviations from long-term averages, making it anomaly-focused, while the normalized map reflects relative magnitudes across the landscape, offering a scale-based interpretation. Together, they provide a robust spatial foundation for the final classification into vegetation–climate response types. / Clear maps shown in the appendix/

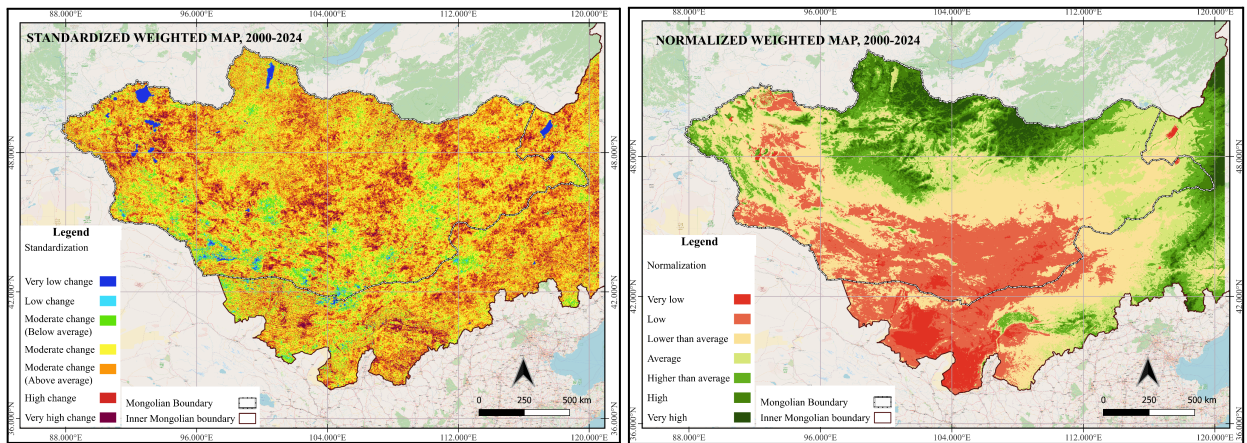


Figure 17. Standardized weighted map

Figure 18. Normalized weighted map

Both standardized and normalized composite maps were classified into categorical ranges to facilitate interpretation of spatial patterns and to distinguish areas by their degree of climate–vegetation variability or condition. The thresholds were determined empirically using frequency histograms, ensuring that the classification scheme reflects the distribution of observed values across the study area.

For the standardized maps, which reflect interannual variability (Z-score-based deviation from long-term means), lower values indicate more stable (i.e., better) conditions, whereas higher values represent increased temporal fluctuation or instability. The classification is as follows:

- Very Low Change: 0.0 – 6.0
- Low Change: 6.0 – 7.0
- Moderate Change (Below Average): 7.0 – 8.0
- Moderate Change (Average): 8.0 – 9.0
- Moderate Change (Above Average): 9.0 – 9.5
- High Change: 9.5 – 10.0
- Very High Change: >10.0

In contrast, the normalized maps, derived through min–max normalization, represent relative vegetation–climate condition magnitudes. Here, higher values indicate better ecological

conditions (e.g., greener, cooler, more humid), and lower values indicate degraded or stressed zones. The normalized classification is:

- Very Low: 0.00 – 0.22
- Low: 0.22 – 0.30
- Below Average: 0.30 – 0.38
- Lower than Average: 0.38 – 0.48
- Higher than Average: 0.48 – 0.60
- High: 0.60 – 0.70
- Very High: >0.70

This classification framework allows for consistent interpretation across maps and supports subsequent response-type analysis and regional comparisons.

3.6 Regional analysis of vegetation–climate response types

To better understand the spatial heterogeneity of climate–vegetation dynamics across the Mongolian Plateau, a regional comparative analysis was conducted. The study area was subdivided into three distinct ecological regions, selected based on their geographic location, geomorphological characteristics, and relevance to land use and economic activity, particularly mining. Each region reflects a different environmental context and serves to illustrate the varying response patterns of vegetation under climate stress.

3.6.1 Transboundary desert regions: Southern Mongolia and Inner Mongolia

The transboundary desert region, spanning southern Mongolia’s Umnugovi Province and neighboring areas of Inner Mongolia’s Alxa League and Bayannur City, represents one of the most environmentally stressed areas in the study.

A total of seven soums from Umnugovi Province were analyzed, including Gurvantes, Noyon, Bayandalai, Nomgon, Khanbogd, Hurmen, and Bayan. From the Inner Mongolian side, the Alxa League comprised nine administrative units, including Ceke, Saihan-Toroi, Dongfeng, Tansagbulag, Olji, Suvnuur, Ontuul, Inggen, and Bayan-Toroi. Additionally, Bayannur City contributed to two areas, Urad Rear Banner and Gaqimaodu town.

3.6.1.1 Normalized composite map results

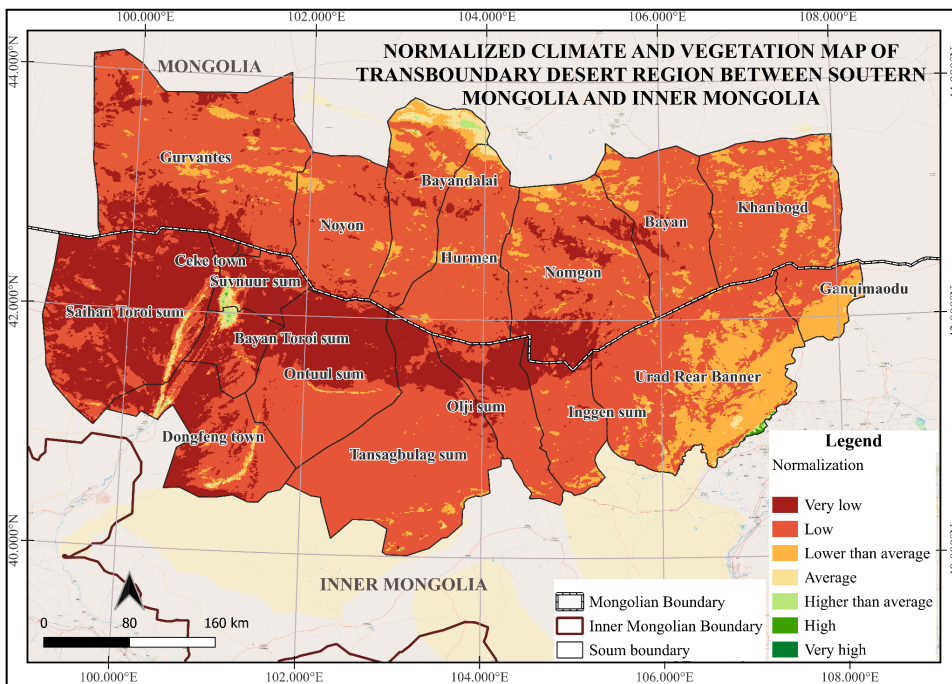
The normalized composite map (Figure 19) illustrates the relative ecological performance within this uniformly arid desert zone. Although all regions fall within the desert classification, significant variation in environmental stress intensity is still evident. A substantial portion of the

area, especially across the central corridor of the border zone, shows “very low” to “low” normalized scores, indicating that these zones perform the worst even within this already dry and degraded landscape.

Key soums and towns, such as Dongfeng, Saihan-Toroi, Bayan-Toroi, Ceke, and Suvnuur, are located in the lowest composite categories, indicating a minimal vegetation response and increased climatic stress, characterized by high LST and ET. These areas are likely experiencing prolonged drought conditions, low soil moisture retention, and increasing land degradation pressure.

Conversely, normalized values ranging from “average” to “above average” were observed in areas such as Urad Rear Banner, Gaqimaodu, Khanbogd, and soums within Bayandalai and Noyon. While still desert, these locations may benefit from relatively favorable microclimates, access to groundwater, or normalized values ranging from “average” to “above average” or stable land management practices.

The normalized results highlight how even within a single desert ecosystem, local-scale differences in climate-vegetation dynamics are detectable. These insights help prioritize zones where ecological resilience exists and areas where intervention is most needed.



/ Clear map shown in the appendix/

Figure 19. Normalized map of the transboundary desert region between southern Mongolia and Inner Mongolia.

3.6.1.2 Standardized composite map results

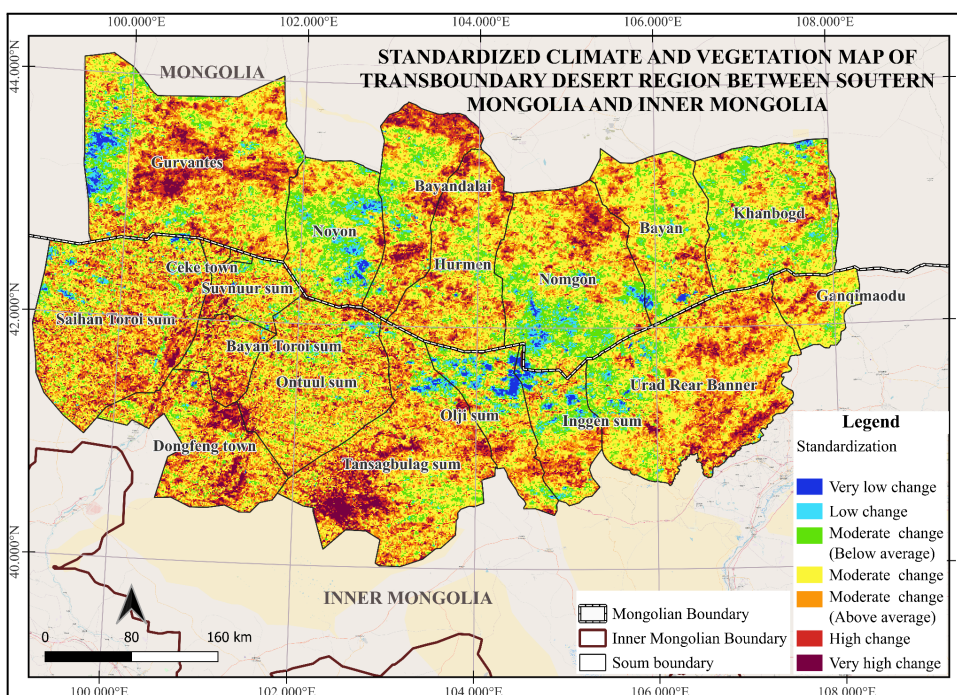
The standardized composite map (Figure 20) reveals the temporal variability in environmental conditions across the transboundary desert region from 2000 to 2024. Unlike the normalized

map, which highlights relative performance, the standardized map emphasizes long-term anomalies, capturing the extent of deviation from historical averages.

Significant deviations were observed in areas such as central and southern Umnugovi (e.g., Gurvantes, Hurmen, northern part of Nomgon) and neighboring regions in Alxa League (e.g., Saihan-Toroi, Dongfeng, Tansagbulag), where higher LST and ET values were paired with lower NDVI, indicating intensifying environmental stress and long-term vegetation decline.

By contrast, soums such as Noyon and Khanbogd, as well as administrative units like Olji and Inggen, displayed lower deviation scores, suggesting relatively stable vegetation and climatic conditions over time. Notably, this desert region demonstrated a higher frequency of minimally changed areas compared to the eastern and northern study regions, despite its harsh baseline environment. This suggests that, despite being inherently low in productivity, many subregions of desert ecosystems have remained climatically and ecologically stable over the past two decades.

This finding highlights an essential ecological nuance, that desert regions can exhibit both high baseline stress and long-term climatic stability, which makes them crucial reference zones for monitoring thresholds of environmental resilience under ongoing climate change.



/ Clear map shown in the appendix/

Figure 20.
Standardized map of the transboundary desert region between southern Mongolia and Inner Mongolia.

3.6.1.3 Classification of vegetation–climate response types

The classification results reveal substantial variation in vegetation–climate response behaviors across the transboundary desert region between southern Mongolia and Inner Mongolia.

Despite the region’s arid environmental baseline, a composite analysis of normalized and standardized values enabled clear differentiation of local response patterns. These were categorized into four vegetation–climate response types, each reflecting varying degrees of productivity, climate stress, and temporal variability.

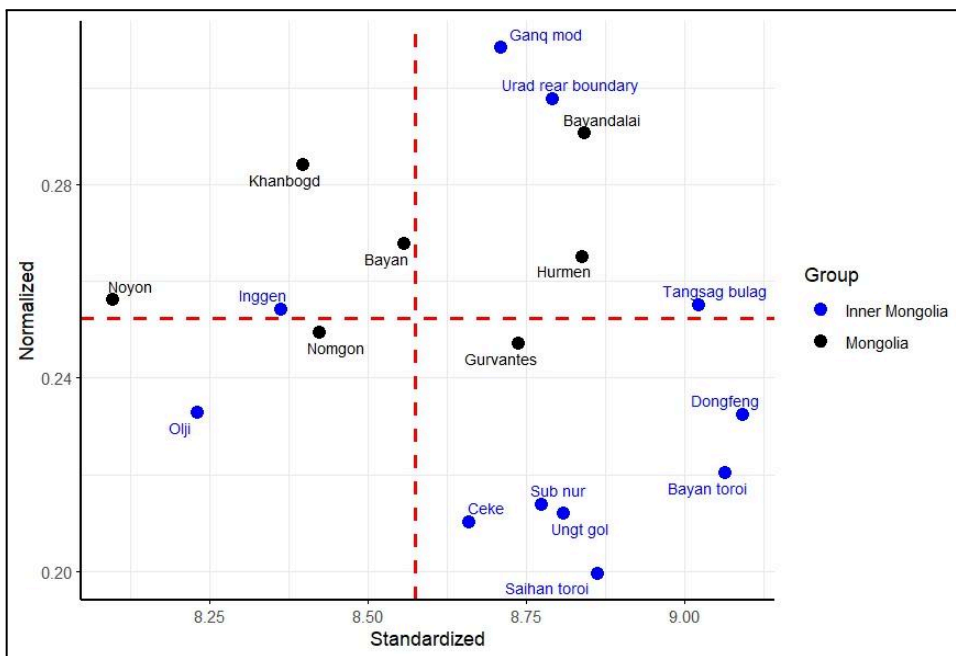


Figure 21. Vegetation–Climate Response Type Classification based on normalized and standardized composite values.

From the scatter plot, vegetation–climate response types were identified for each soum and town in the study area based on their relative positions across standardized and normalized axes, allowing the classification of local conditions into four distinct environmental response categories.

Table 13. Vegetation–Climate Response Classification of Soums in Southern Mongolia (Colored by Response Type)

	Low interannual deviation	High interannual deviation
High vegetation and low LST&ET	Noyon, Inggen, Khanbogd, Bayan	Ganqimaodu, Urad Rear boundary, Bayandalai, Hurmen, Tansagbulag,
Low vegetation and high LST&ET	Olji, Nomgon	Gurbantes, Dongfeng, Suvnuur, Ontuul, Ceke, Bayan toroi, Saihan toroi

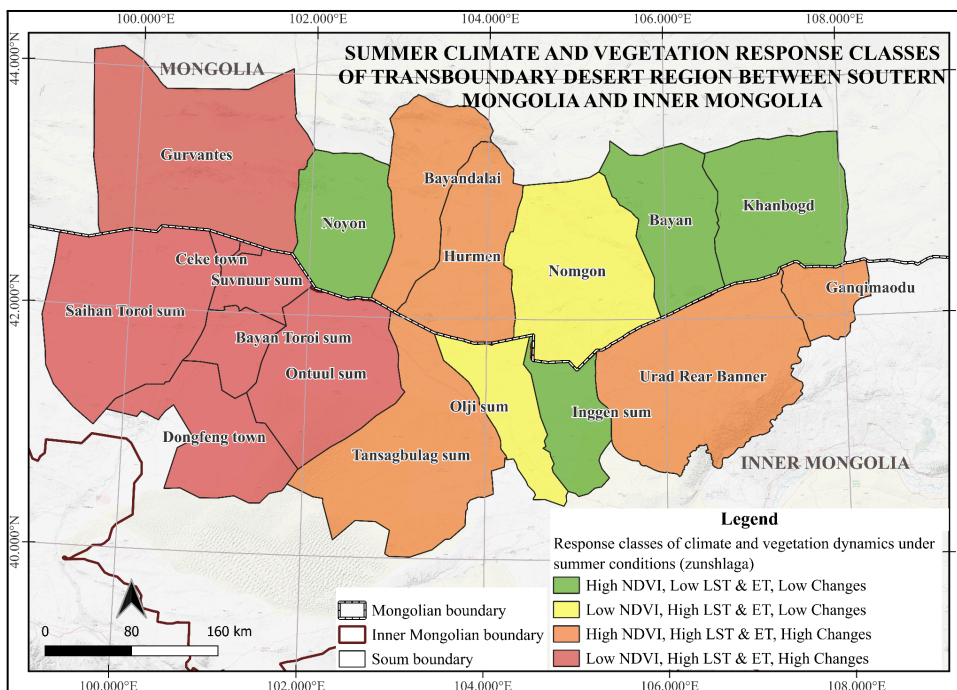
Among these, Type IV was the most dominant, covering approximately 37.8% of the study area. This group includes Gurvantes, Dongfeng, Suvnuur, Ontuul, Ceke, Bayan-Toroi, and Saihan-Toroi. These areas exhibit low NDVI values, high LST and ET levels, and high interannual variability, indicating extreme environmental degradation and instability.

Type III accounts for 32.3% of the area and includes Ganqimaodu, Urad Rear Banner, Bayandalai, Hurmen, and Tansagbulag. These areas show relatively high vegetation productivity but also experience high temporal variability, suggesting sensitive yet currently functional ecosystems.

Type II represents 11.4% of the study region and includes Olji and Nomgon. These locations show low vegetation productivity combined with relatively stable climate indicators, likely representing inherently arid or slowly degrading landscapes.

Type I covers 19.0% of the area, including Noyon, Inggen, Khanbogd, and Bayan. These areas exhibit high NDVI, low climate stress, and minimal year-to-year variability, indicating localized ecological stability or effective land management.

Spatial patterns are further illustrated in the classification map (Figure 22), which shows the geographic distribution of each response type across the study area.



/ Clear map shown in the appendix/

Figure 22. Spatial distribution of response types across the transboundary desert region.

3.6.2 Transboundary steppe and regions: Eastern Mongolia and Inner Mongolia

The transboundary steppe region, spanning eastern Mongolia's Dornod Province and adjacent areas of Inner Mongolia's Hulunbuir and Xilin Gol Leagues, forms one of the ecologically transitional zones in this study.

A total of six soums from Dornod Province were analyzed: Gurvanzagal, Choibalsan, Chuluunkhoroot, Herlen (the provincial capital), Matad, and Halhgal.

On the Inner Mongolian side, the study includes administrative units from both Hulunbuir City and the Xilin Gol League. This consists of the New Barag Left Banner and New Barag Right Banner in Hulunbuir, as well as Bogd Town, Mandahbulag Town, Samai, and Gahail sums from Xilin Gol.

Together, these cross-border zones form a critical ecological corridor where the intersection of grassland productivity, climate resilience, and transboundary land-use dynamics is evident. This section examines the climate–vegetation response behavior in this region, focusing on spatial differences, stability trends, and degradation risks.

3.6.2.1 Normalized composite map results

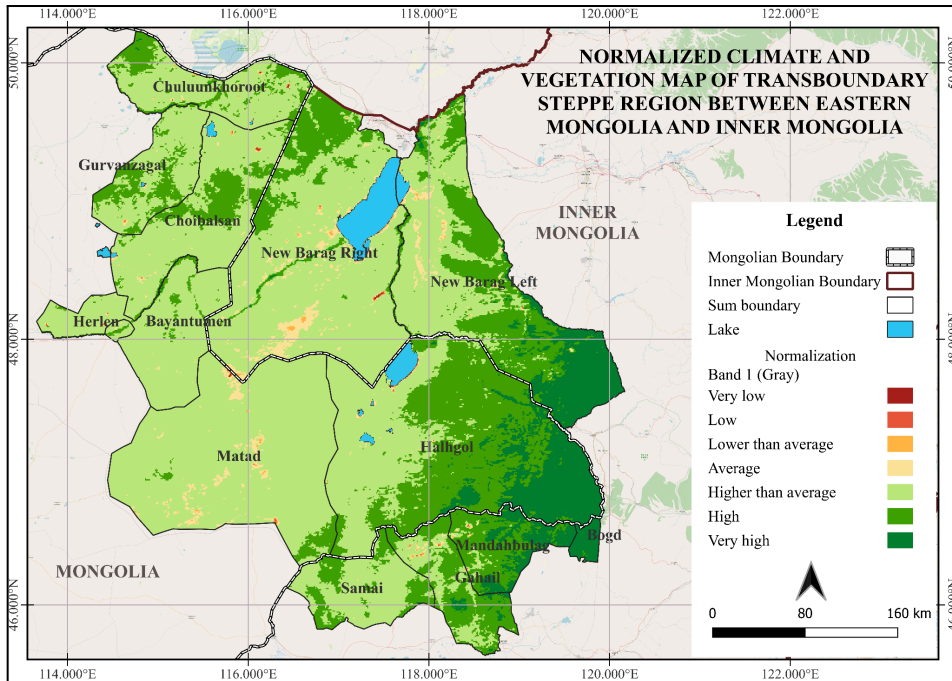
The Normalized Climate and Vegetation Map (Figure 23) illustrates the relative ecological performance of each soum and town within the transboundary steppe and forest steppe region. In contrast to the arid desert zones, this area generally exhibits higher vegetation productivity, with large parts of the study area classified as “average” to “very high” in terms of normalized values.

The Inner Mongolian side, particularly New Barag Left Banner, Samai, Mandahbulag, Gahail, and Bogd, shows mostly “above average” to “very high” normalized values. This reflects strong vegetation performance, likely supported by favorable rainfall, cooler surface temperatures, and intact grassland ecosystems. These areas represent some of the most ecologically productive zones across the entire study area.

On the Mongolian side, soums such as Gurvanzagal, Chuluunkhoroot, Bayantümen, Halhgal, and Herlen fall primarily into the “average” to “higher than average” categories. Eventhough Matad displays spatial variability, with zones ranging from “lower than average” to “high”, indicating diverse micro-conditions within the soum, possibly driven by land use and grazing intensity. This suggests that the region maintains overall ecological resilience, although local

stress may be emerging in areas such as the New Barag Right Banner, located along the western side of Hulunbuir City in Inner Mongolia.

In summary, the normalized results confirm that the eastern steppe and forest steppe zone is significantly more vegetated and climatically favorable than southern desert areas. However, monitoring should continue, especially in transitional zones and areas with high pasture use.



/ Clear map shown in the appendix/

Figure 23. Normalized map of the transboundary desert region between eastern Mongolia and Inner Mongolia.

3.6.2.2 Standardized composite map results

The Standardized Climate and Vegetation Map (Figure 24) illustrates the extent of temporal variability in vegetation and climate conditions across the eastern transboundary steppe and forest steppe region, spanning Mongolia and Inner Mongolia. This map illustrates the degree to which each location deviated from its long-term mean during the 2000–2024 period, indicating whether it experienced climatic and ecological stability or instability over time.

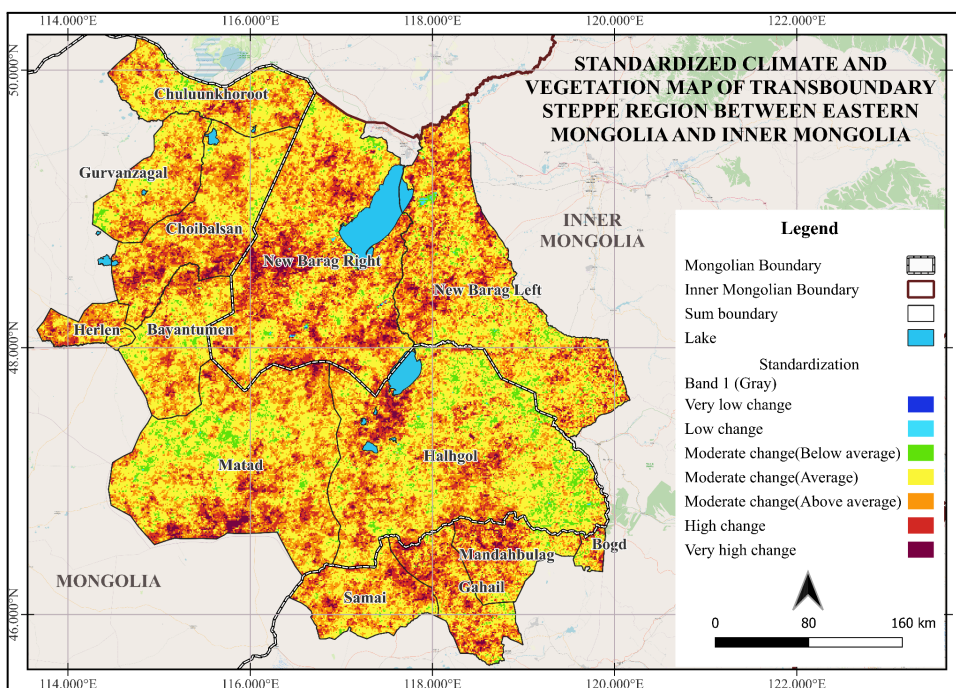
A crucial pattern in the standardized results is the high interannual variability observed across much of the region. Areas such as New Barag Right Banner, Choibalsan, Gahail and Mandahbulag display extensive zones of high to very high deviation, suggesting persistent ecological fluctuations likely tied to climate stress, land use intensity, or both. These fluctuations may reflect the growing vulnerability of central grazing corridors in the steppe zone.

On the other hand, New Gurvanzagal, Halhgoi, the northwestern side of Matad, and Bogd exhibit larger patches of below-average to high change. These areas have exhibited slow degradation or stable vegetation and climate change over the past 25 years, likely due to

moderate vegetation cover and proximity to water bodies. However, even within these zones, localized hotspots of change exist.

Matad, in particular, exhibits diverse patterns, with some areas experiencing low to moderate change, while others display higher deviations, which may reflect varying ecological pressures across its broad steppe area.

The overall picture suggests that, while the normalized values highlight firm productivity, the standardized map reveals underlying instability, which is almost all over the region, except in certain areas. This contrast underscores the importance of combining both metrics to identify not only where vegetation is strong but also where it is vulnerable to disruption.



/ Clear map shown in the appendix/

Figure 24. Standardized map of the transboundary desert region between eastern Mongolia and Inner Mongolia.

3.6.2.3 Classification of vegetation–climate response types

The classification of vegetation–climate response types for the eastern steppe and forest steppe region highlights a more balanced ecological structure compared to the southern desert zone, with relatively stable and productive areas coexisting alongside emerging hotspots of degradation. The quadrant-based analysis using standardized and normalized values allowed each soum and town to be assigned to one of four response types.

The response types are visualized in Figures 25 (scatter plot) and 26 (spatial classification map). These tools provide a comprehensive perspective on the intersection of climate and vegetation dynamics, offering a decision-making foundation for transboundary environmental planning and monitoring efforts.

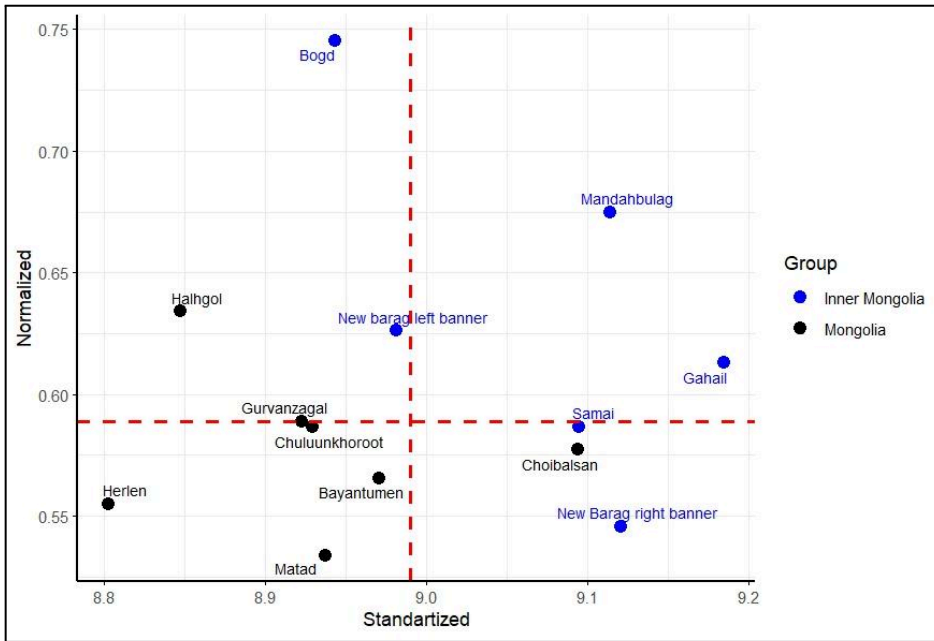


Figure 25. Vegetation–Climate Response Type Classification of the transboundary steppe region between eastern Mongolia and Inner Mongolia.

Table 14. Vegetation–Climate Response Classification of Soums in Eastern Mongolia (Colored by Response Type)

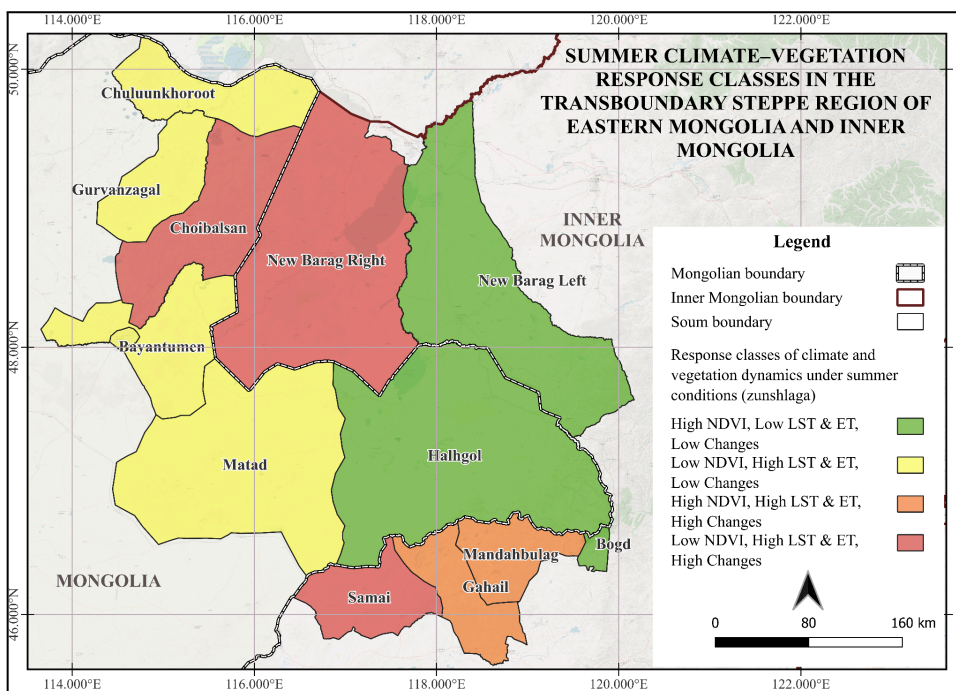
	Low interannual deviation	High interannual deviation
High vegetation and low LST&ET	Halhgoi, Bogd, New Barag Left Banner	Mandahbulag, Gahail
Low vegetation and high LST&ET	Chuluunkhoroot, Bayantumen, Matad, Herlen, Gurvanzagal	Choibalsan, New Barag Right Banner

Type I covered 34.0% of the area and included locations such as New Barag Left Banner, Halhgoi, and Bogd. These zones are characterized by high vegetation productivity, low land surface temperature and evapotranspiration, and minimal interannual variability. Their combination of strong ecological performance and stability suggests they may serve as reference areas or resilience cores within the broader steppe zone.

Type II accounted for 30.2% and includes soums such as Gurvanzagal, Chuluunkhoroot, Herlen, Bayantumen, and Matad. These areas exhibit lower vegetation performance under relatively stable climatic conditions. Although not experiencing large fluctuations, their long-term ecological baseline remains low, indicating a gradual degradation or inherent productivity limitations in certain parts of the steppe.

Type III was less common, representing 7.0% of the region and includes Gahail and Mandahbulag. These areas exhibit high vegetation productivity but display notable interannual variation, suggesting sensitive yet functional ecosystems that could shift toward instability if climate stressors intensify.

Type IV made up 28.8% of the region and included Choibalsan, New Barag Right Banner, and Samai. These areas combine low vegetation indices with high temporal variability, indicating that they are subject to both high degradation and climate-induced stress. These locations are the most vulnerable and may require immediate attention or intervention in land management.



/ Clear map shown in the appendix/

Figure 26. Spatial distribution map of vegetation-climate response types of the transboundary steppe region between eastern Mongolia and Inner Mongolia

3.6.3 Northern regions of Mongolia: Selenge and Darkhan provinces

The northern part of the study area encompasses the entire administrative territories of Selenge and Darkhan-Uul Provinces, covering 21 soums. Located in Mongolia’s forest steppe and agricultural belt, this region represents one of the country’s most ecologically productive and densely vegetated areas. It is also one of Mongolia’s key zones for crop farming, pasture use, and river-based ecosystems, supported by major watercourses like the Selenge, Orkhon, and Kharaa rivers.

This section evaluates the long-term vegetation and climate dynamics of the northern region by analyzing normalized and standardized composite indicators for all soums in Selenge and Darkhan-Uul Provinces, followed by classification into four vegetation–climate response types.

The findings offer critical insights into both the resilience and emerging risks in Mongolia's most agriculturally and ecologically strategic region.

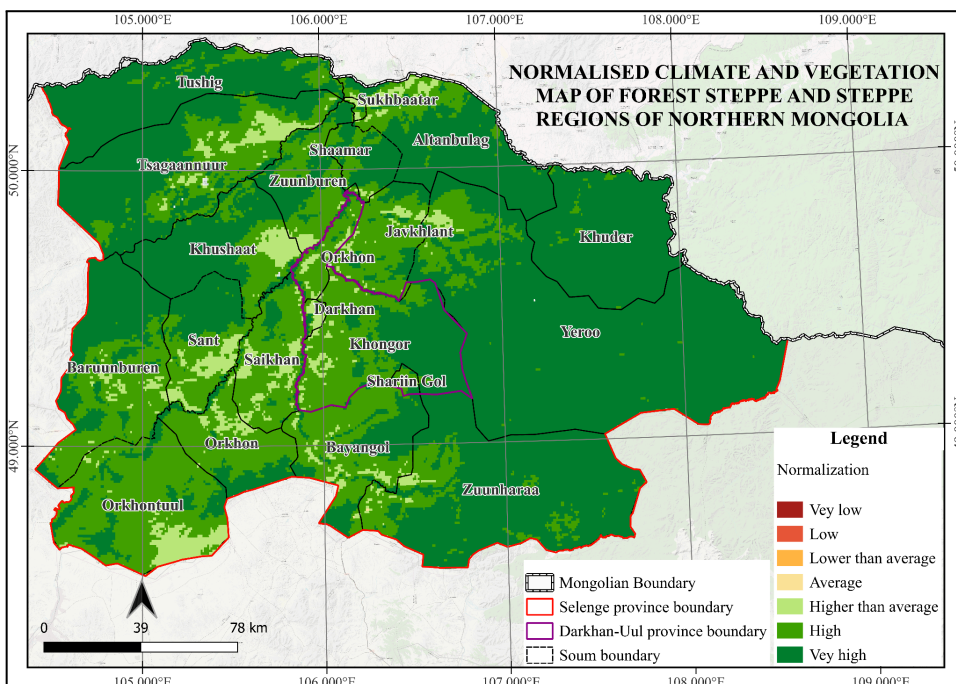
3.6.3.1 Normalized composite map results

The Normalized Climate and Vegetation Map (Figure 27) reveals consistently high ecological productivity across the entire northern region, comprising all soums of Selenge and Darkhan-Uul Provinces. Most of the territory is classified as “higher than average,” “high,” or “very high”, reflecting the region’s favorable climatic conditions and rich vegetation cover.

The eastern and central parts of Selenge Province, including Yeroo, Khuder, Altanbulag, Shaamar, and Tushig soums, exhibit very high normalized values, indicating stable, well-performing vegetation systems. These areas benefit from proximity to rivers, forested zones, and a humid microclimate, which supports the growth of dense vegetation.

The southern parts of Selenge and the Darkhan-Uul region, including Baruunburen, Orkhon, Khongor, Bayangol, Javkhiant, and Zuunkharaa, also exhibit mostly high to very high values, indicating a healthy vegetation cover even in agriculturally intensive zones. Slightly more moderate values are observed in the Orkhon(Selenge), Khushaat, Orkhontuul, Saikhan, and Tsagaannuur soums, but they still fall within the range of above-average productivity.

Notably, no significant zones of low or very low normalized values are present in the region, making it the strongest-performing zone among all three major regions in the study. This map confirms that northern Mongolia is characterized by dense vegetation and a relatively stable environment. However, it does not capture the underlying climatic variability, which is addressed in the next section.



/ Clear map shown in the appendix/

Figure 27. Normalized map of the forest steppe regions of northern Mongolia

3.6.3.2 Standardized composite map results

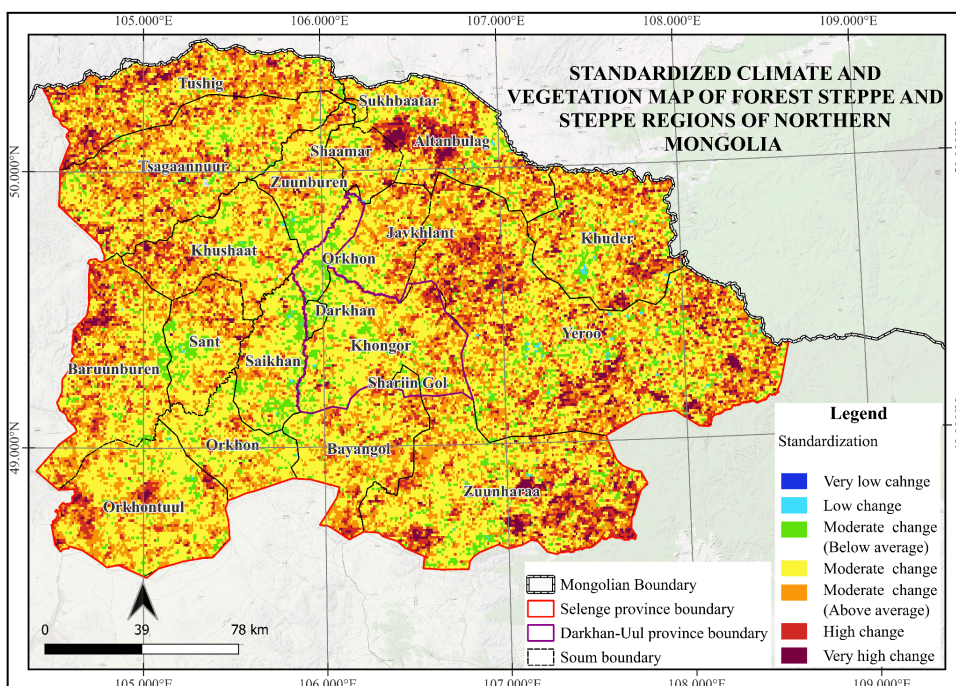
The Standardized Climate and Vegetation Map (Figure 28) highlights the interannual variability of NDVI, LST, and ET values across the northern provinces over the 2000–2024 period. While the normalized map showed widespread ecological strength, the standardized map reveals a more complex picture, with significant spatial variation in environmental stability.

Notably, many areas throughout central and eastern Selenge, such as Shaamar, Altanbulag, Khuder, and parts of Yeroo, exhibit zones of high and very high variability, suggesting fluctuations in surface temperature, vegetation health, and evapotranspiration rate. These areas may be vulnerable to short-term climatic fluctuations, such as droughts or extreme rainfall events.

In contrast, soums such as Sant, Saikhan, Orkhon, and Baruunburen exhibit broader regions of low to moderate change, indicating stable long-term ecological conditions. These areas, along with central parts of Darkhan and Khongor, are less affected by abrupt year-to-year environmental changes, potentially due to better moisture retention, forest cover, or lower land-use pressure.

Interestingly, the southern border zone, particularly Zuunharaa, Bayangol, and parts of Orkhontuul, also exhibits higher deviation zones, possibly reflecting a transition between forest steppe and agricultural land, where human activity and climate pressures intersect.

Overall, while the northern region remains the most ecologically productive in the country, the standardized results reveal emerging instability in specific sub-regions. These findings emphasize the importance of combining both normalized strength and standardized stability when assessing long-term climate–vegetation dynamics.



/ Clear map shown in the appendix/

Figure 28. Standardized map of the forest steppe regions of northern Mongolia

3.6.3.3 Classification of vegetation–climate response types

The classification of vegetation–climate response types in the northern region, covering all soums of Selenge and Darkhan-Uul Provinces, reveals a diverse ecological landscape shaped by both climatic variability and land-use intensity. While most of the region exhibits a high density of vegetation, the standardized and normalized composite analysis reveals climate and vegetation dynamics under summer conditions (*zunshlaga*).

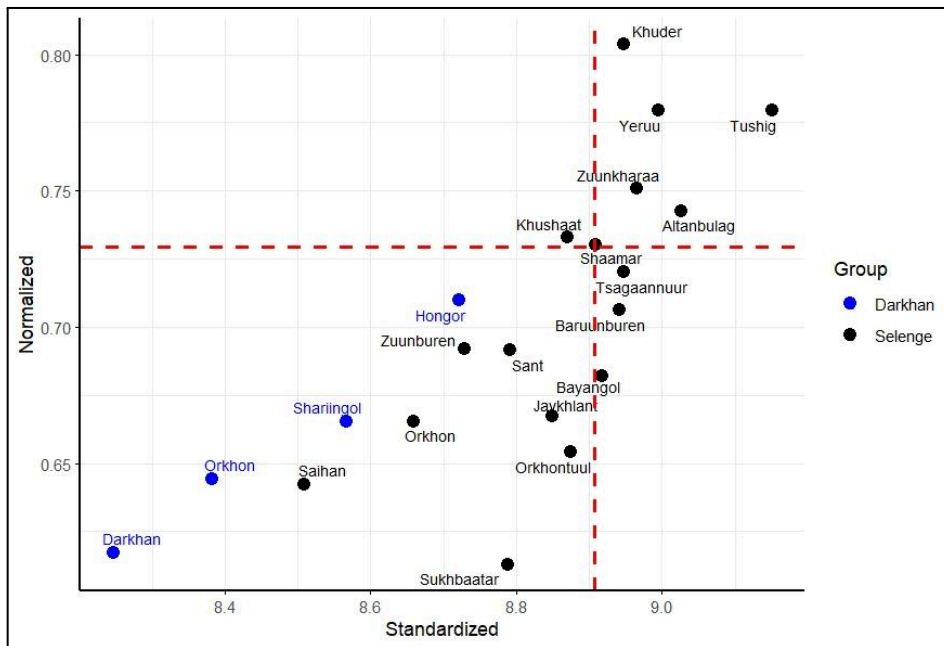


Figure 29. Vegetation–Climate Response Type Classification of the forest steppe regions of northern Mongolia

From the scatter plot (Figure 29), it is evident that the northern region generally experiences favorable summer conditions (*zunshlaga*), as reflected in the average to very high normalized values across all soums. However, some areas still fall below the regional mean, indicating that they perform worse than the average for Selenge and Darkhan-Uul, with relatively lower NDVI values and higher LST and ET. This may indicate targeted ecological stress or limited vegetation response despite the overall climatic advantage. Such deviations could be attributed to factors such as soil degradation, land use intensity, or microclimatic variability.

Table 15. Vegetation–Climate Response Classification of Soums in Northern Mongolia (Colored by Response Type)

	Low interannual deviation	High interannual deviation
High vegetation and low LST&ET	Khushaat	Khuder, Yeruu, Zuunkharaa, Altanbulag, Tushig
Low vegetation and high LST&ET	Saihan, Orkhon (Selenge) Sant, Zuunburen, Orkhon (Darkhan) Orkhontuul, Sukhbaatar, Javkhlant, Darkhan, Shariin gol, Orkhon, Khongor	Tsagaannuur, Baruunburen, Bayangol

Type I is the least represented category, accounting for only 4.5% of the region. Found primarily in Khushaat soum, these areas exhibit high vegetation performance, low climatic stress, and minimal year-to-year change. These zones serve as rare but valuable examples of ecosystem resilience and may provide local benchmarks for sustainable land use and conservation.

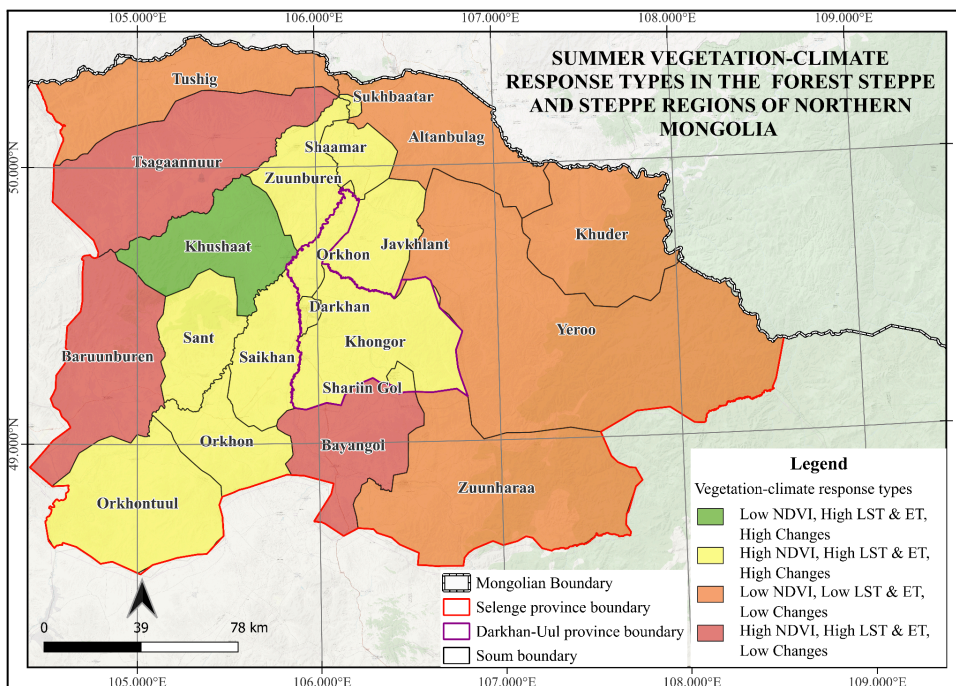
Type II, representing 29.5% of the area, includes Saikhan, Orkhon (Selenge) Sant, Zuunburen, Orkhon (Darkhan) Orkhontuul, Sukhbaatar, Javkhlant, Darkhan, Shariin gol, Orkhon, and Khongor. These areas exhibit lower vegetation productivity (low NDVI) and higher climatic stress (high LST and ET), but they have shown relative stability over the years. The persistence of low vegetation under stable climatic conditions suggests long-term ecological degradation, possibly due to land-use pressure, overgrazing, or soil exhaustion.

Type III is the most dominant category, comprising 46.7% of the area. This group comprises many of the productive yet climate-sensitive soums, including Tushig, Altanbulag, Khuder, Yeroo, and Zuunkharaa. They are characterized by high NDVI values and low land surface temperature and evapotranspiration, but also exhibit substantial interannual deviation. This indicates strong vegetation health under conditions of temporal climatic instability. These soums may be sensitive to climatic anomalies, where fluctuations in rainfall or temperature could affect long-term ecological resilience.

Type IV accounts for 19.3% of the region and includes locations such as Bayangol, Baruunburen, and Tsagaannuur. These areas combine low vegetation productivity with high interannual variability, making them particularly vulnerable to environmental stress. This pattern

reflects ecosystems under compounded pressure from both human activity and climate variability, underscoring the need for enhanced monitoring and interventions. This group represents a key zone for land management attention and climate adaptation.

Together, the results emphasize the importance of combining both vegetation magnitude (normalized values) and temporal variability (standardized values) to interpret regional ecological performance. This dual-metric approach reveals not only where ecosystems are strong but also where they are fragile or in decline, offering valuable insights for regional planning, adaptation strategies, and assessments of ecosystem resilience.



/ Clear map shown in the appendix/

Figure 30. Spatial distribution map of vegetation-climate response types of the forest steppe regions of northern Mongolia

4. Recommendation based on regional analysis of vegetation–climate response types

Based on the vegetation–climate response classification across the three ecologically distinct regions of the Mongolian Plateau, several region-specific and general recommendations are proposed to enhance ecological resilience, mitigate environmental degradation, and support sustainable land-use strategies.

In the transboundary desert region of Southern Mongolia and Inner Mongolia, where most areas fall into Type IV (low vegetation, high LST and ET, and high interannual variability), urgent measures are needed to counteract severe environmental degradation. These areas, such as Gurvantes, Dongfeng, Suvnuur, and Bayan-Toroi, should be prioritized for land rehabilitation

programs, including the implementation of erosion control techniques, the introduction of drought-tolerant native plant species, and the development of localized water management systems to enhance soil moisture retention. Meanwhile, Type I areas like Khanbogd, Noyon, and Inggen, which show ecological stability, should be designated as ecological reference zones and preserved through minimal disturbance policies and regular monitoring to track potential stress signals.

In the **eastern steppe and forest-steppe region**, which displays a more balanced distribution across all four response types, attention should be given to areas under Type IV (e.g., Choibalsan, New Barag Right Banner, Samai) and Type III (e.g., Gahail, Mandahbulag) classifications. These zones are ecologically productive but climatically unstable, highlighting the need for adaptive grazing systems, enforcement of rotational land use, and transboundary cooperation for rangeland protection. Type I zones like Halhgal and Bogd should be maintained as resilience hubs through ecosystem service payments or conservation incentives, while Type II regions can benefit from improved land-use practices to gradually restore vegetation cover and reduce pressure from grazing and land conversion.

The **northern forest-steppe region**, encompassing Selenge and Darkhan provinces, demonstrated high ecological productivity but emerging instability in specific subregions. Although the Type I area Khushaat remains ecologically stable, nearly half of the region was categorized as Type III, reflecting high productivity but increasing sensitivity to climatic fluctuations. These productive yet fragile ecosystems, such as Tushig, Khuder, and Yeroo, require investment in sustainable agroforestry practices, soil moisture conservation techniques, and crop diversification to buffer against interannual climate variability. Meanwhile, Type IV zones like Tsagaannuur and Bayangol warrant targeted soil stabilization efforts, reforestation near water bodies, and stricter control of land-use intensity to prevent further degradation.

5. Conclusion

This study assessed long-term climate and vegetation dynamics across selected regions of the Mongolian Plateau by integrating satellite-derived indicators NDVI, LST, and ET, using standardized and normalized raster analyses. Composite indices were developed by applying the Analytic Hierarchy Process (AHP) for parameter weighting and spatial overlay techniques in GIS to reflect both absolute environmental conditions and interannual variability. These indices enabled the classification of all study areas into four Vegetation–Climate Response Types (VCRT), providing a robust framework for understanding ecological resilience and vulnerability under ongoing climatic shifts.

The results revealed considerable spatial heterogeneity in ecosystem responses across the plateau. Despite harsh climatic baselines, the southern desert regions displayed both extreme degradation and surprising stability in localized zones, underscoring the need for targeted interventions and preservation of micro-resilient ecosystems. The **eastern steppe regions** showed stronger vegetation productivity but experienced high temporal variability, suggesting emerging risks due to land-use pressure and climate extremes. Meanwhile, the **northern forest-steppe region**, particularly in Selenge and Darkhan-Uul provinces, exhibited overall high ecological productivity. However, a deeper analysis revealed areas of increasing fluctuation and vulnerability, emphasizing that even the most productive ecosystems require careful management to maintain long-term stability.

This research provides a nuanced basis for environmental decision-making by classifying the study regions into VCRT categories. Type I areas, like Khushaat soum in Selenge, represent ecological benchmarks that should be preserved and studied as models of resilience. Conversely, Type IV areas demand urgent restoration efforts and policy interventions. The methodological framework, combining MODIS satellite data, multivariate index construction, and spatial classification, demonstrates the utility of remote sensing for landscape-level monitoring and environmental planning in data-scarce regions.

Overall, this study contributes valuable insight into the intersection of climate change and vegetation dynamics in the Mongolian Plateau. The findings offer both a scientific foundation and a practical toolset for sustainable land management, climate adaptation, and long-term ecological monitoring. Future work may build upon this foundation by incorporating socio-economic data, modeling future climate scenarios, and expanding monitoring efforts to additional regions for a more comprehensive assessment of the Plateau's ecological trajectory.

References

1. Yanzhen Zhang, Qian Wang, Zhaoqi Wang, Yue Yang, Jianlong Li. Impact of human activities and climate change on the grassland dynamics under different regime policies in the Mongolian Plateau. *Science of The Total Environment*. 2020;698. Available from: doi:10.1016/j.scitotenv.2019.134304
2. Dash Doljin, Batchuluun Yembuu. The Relief and Geomorphological Characteristics of Mongolia. *Geography of the Physical Environment*. 2021:23–50 Available from: https://doi.org/10.1007/978-3-030-61434-8_3
3. Ranjeet John, Jiquan Chen, Zu-Tao Ou-Yang, Jingfeng Xiao, Richard Becker, Arindam Samanta, et.al. Vegetation response to extreme climate events on the Mongolian Plateau from 2000 to 2010. *Environmental Research Letters*. 2013;8
4. Batjargal.Z. Global climate change and its regional and local implications. *Mongolia Second Assessment Report on Climate Change 2014*. 2014;2:51-52
5. Grainger A. Is Land Degradation Neutrality feasible in dry areas?. *Journal of Arid Environments*. 2015;112:14-24 Available from: <https://doi.org/10.1016/j.jaridenv.2014.05.014>.
6. Lin, Y., Han, G., Zhao, M., Chang, S. Spatial vegetation patterns as early signs of desertification: a case study of a desert steppe in Inner Mongolia, China. *Landscape Ecology*. 2010;25:1519–1527 Available from: <https://doi.org/10.1007/s10980-010-9520-z>
7. Cao, X., Feng, Y. & Shi, Z. Spatio-temporal Variations in Drought with Remote Sensing from the Mongolian Plateau During 1982–2018. *Chinese Geographical Science*. 2020;30:1081–1094 Available from: <https://doi.org/10.1007/s11769-020-1167-3>
8. Bari, E., Nipa, JN, Roy, B. Association of Vegetation Indices with Atmospheric & Biological Factors Using MODIS Time Series Products. *Environmental Challenges*. 2021;5. Available from: <https://doi.org/10.1016/j.envc.2021.100376>.
9. Yengoh, G. T., Dent, D., Olsson, L., Tengberg, A. E., & Tucker III, C. J. Use of the Normalized Difference Vegetation Index (NDVI) to Assess Land Degradation at Multiple Scales. *SpringerBriefs in Environmental Science*, Cham, Springer International Publishing, 2016:11-17
10. Pettorelli N, Vik JO, Mysterud A, Gaillard JM, Tucker CJ and Stenseth NC. Using the satellite-derived NDVI to assess ecological responses to environmental change. *Trends in Ecology and Evolution*. 2005;20(9):503–510. Available from: <https://doi.org/10.1016/j.tree.2005.05.011>

11. Bao G, Qin Z, Bao Y, Zhou Y, Li W, Sanjjav A. NDVI-Based Long-Term Vegetation Dynamics and Its Response to Climatic Change in the Mongolian Plateau. *Remote Sensing*. 2014;6(9):8337-8358; Available from: <https://doi.org/10.3390/rs6098337>
12. Meng M, Huang N, Wu M, Pei J, Wang J, Niu Z. Vegetation change in response to climate factors and human activities on the Mongolian Plateau. 2019 Available from: <https://doi.org/10.7717/peerj.7735>
13. Guha S, and Govil H. Land surface temperature and normalized difference vegetation index relationship: a seasonal study on a tropical city. *SN Applied Sciences*, 2020;2 Available from: doi:10.1007/s42452-020-03458-8
14. Tuya S, Nandin-Erdene G, Lkhagvadorj N, Damdinpurevnyam M, Oyun R . The base research results of Mongolia's environmental and climatic conditions and changes, based on satellite data from 2000 to 2023, focus on the Dornod and Sukhbaatar provinces. *Erdmiin Chuulgan 2023*. 2023:126-129
15. Sixth Assessment Report: Impacts, Adaptation, and Vulnerability. Intergovernmental Panel on Climate Change. 2022;1459-2532
16. Yanfei M, Zhou J, Liu S, Zhang W, Zhang Y, Xu Z, et.al. Estimation of Evapotranspiration Using All-Weather Land Surface Temperature and Variational Trends with Warming Temperatures for the River Source Region in Southwest China. *Journal of Hydrology*, 2022;613:128346. Available from: <https://doi.org/10.1016/j.jhydrol.2022.128346>.
17. Cihlar J, St.-Laurent L, Dyer D.A. Relation between the Normalized Difference Vegetation Index and Ecological Variables. *Remote Sensing of Environment*, 1991;35(2-3): 279–298, Available from: [https://doi.org/10.1016/0034-4257\(91\)90018-2](https://doi.org/10.1016/0034-4257(91)90018-2).
18. Liu, Y., Q. Zhuang, M. Chen, Z. Pan, N. Tchebakova, A. Sokolov, D. Kicklighter, et, al. Response of evapotranspiration and water availability to changing climate and land cover on the Mongolian Plateau during the 21st century. *Global and Planetary Change*. 2013;108:85–99. Available from: <http://dx.doi.org/10.1016/j.gloplacha.2013.06.008>
19. Jiang L, Yao Z, Huang HQ. Climate variability and change on the Mongolian Plateau: historical variation and future predictions. *Climate Research*. 2016;67:1-14. Available from:<https://doi.org/10.3354/cr01347>
20. Bolortsetseg B, Tuvaansuren G. The potential impacts of climate change on pasture and cattle production in Mongolia. *Water Air, and Soil Pollution*. 1996;92 95–105. Available from: <https://doi.org/10.1007/BF00175556>
21. Lkhamjav, O., Batbold, U., Renchinmyag, D., Ulziibat, B., Enkhtaivan, U., Erdenegerel, A., et, al. The Progress/Status of Ecological Assessment on the Intensive Land Use in Selenge and Darkhan-Uul Province, Mongolia. *Intelligent Sensing and Remote Sensing*

Application. 2024;48:437-437. Available from:
<https://doi.org/10.5194/isprs-archives-XLVIII-1-2024-437-2024>

22. Lkhamjav O, Uyanga B, Bilguun U, Uuriintsolmon E, Ariunbold E, Khaulanbek A. Using geo-spatial data and dataset for cropland monitoring in Darkhan-Uul and Selenge provinces, Mongolia. *Remote Sensing and Spatial Information Sciences.* 2023;48:451-456. Available from: [10.5194/isprs-archives-XLVIII-1-W2-2023-451-2023](https://doi.org/10.5194/isprs-archives-XLVIII-1-W2-2023-451-2023)
23. Saaty T.L. The analytic hierarchy process-what it is and how it is used. *Mathematical Modelling.* 1987;9(3-5):161-176. Available from:[https://doi.org/10.1016/0270-0255\(87\)90473-8](https://doi.org/10.1016/0270-0255(87)90473-8)
24. Saaty, T. L. How to make a decision: The Analytic Hierarchy Process. *European Journal of Operational Research,* 1990;48(1):9–26. Available from: [https://doi.org/10.1016/0377-2217\(90\)90057-I](https://doi.org/10.1016/0377-2217(90)90057-I)
25. Rao R.V. Decision Making in the Manufacturing Environment: Using Graph Theory and Fuzzy Multiple Attribute Decision Making Methods chapter Multiple Attribute Decision-making Methods. 2007:29-32

Appendix

Figure 4

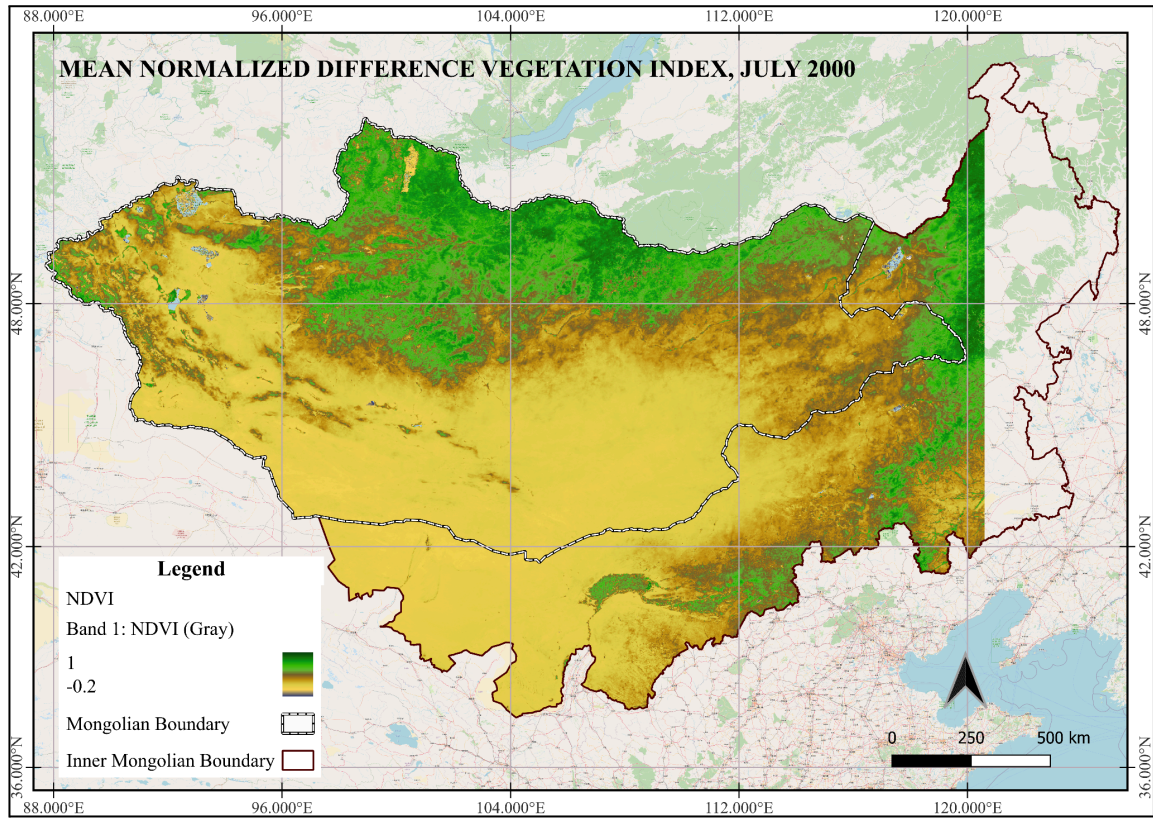


Figure 5

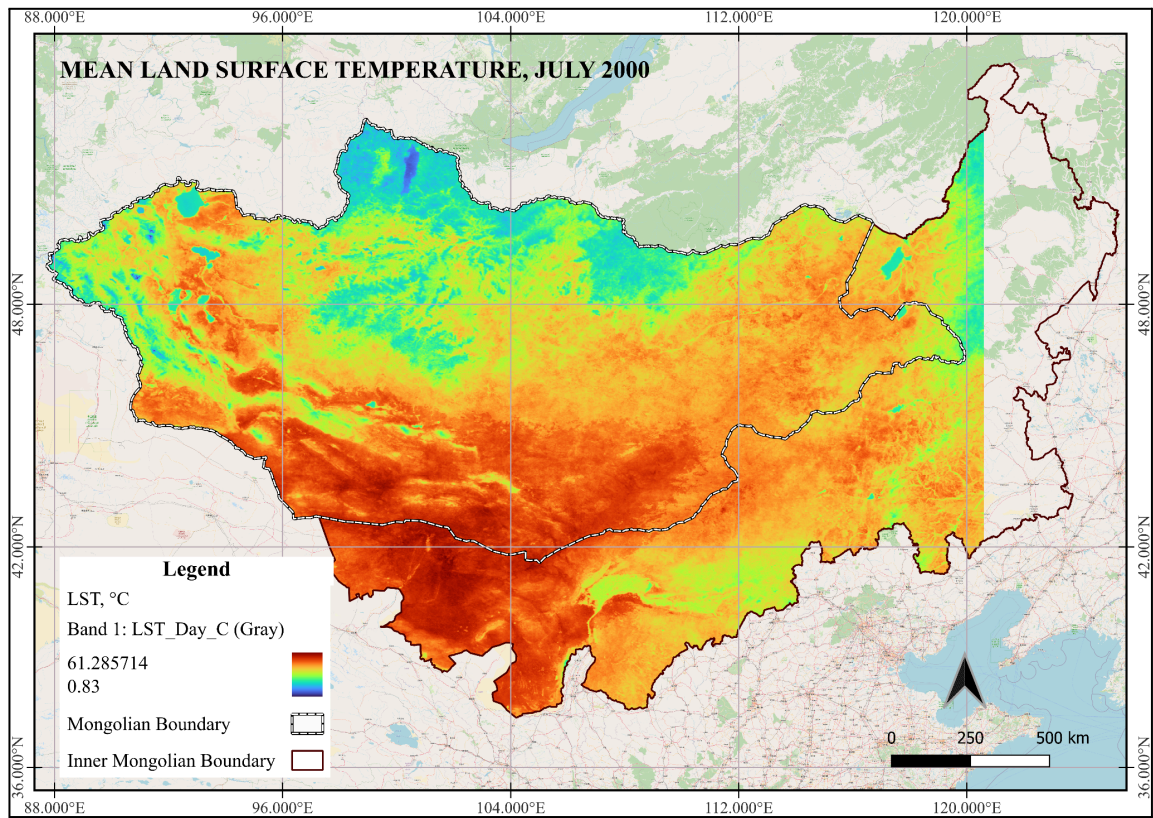


Figure 6

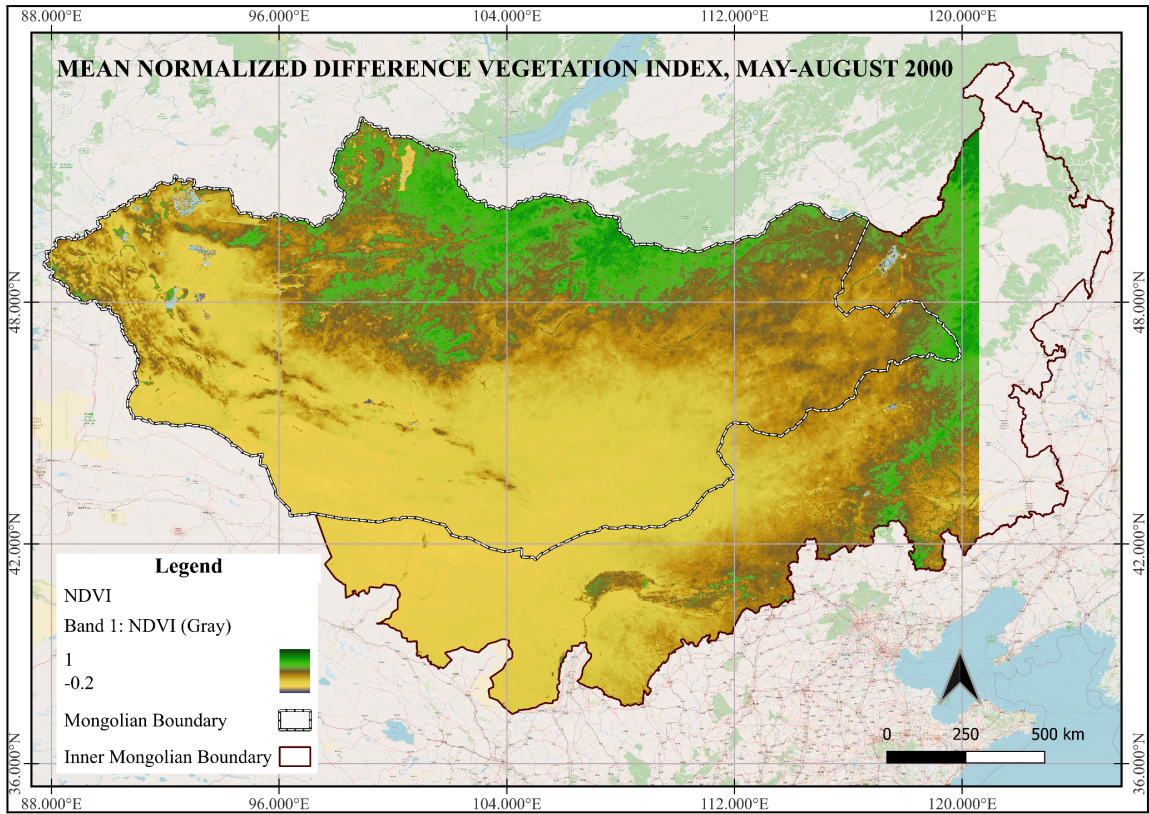


Figure 7

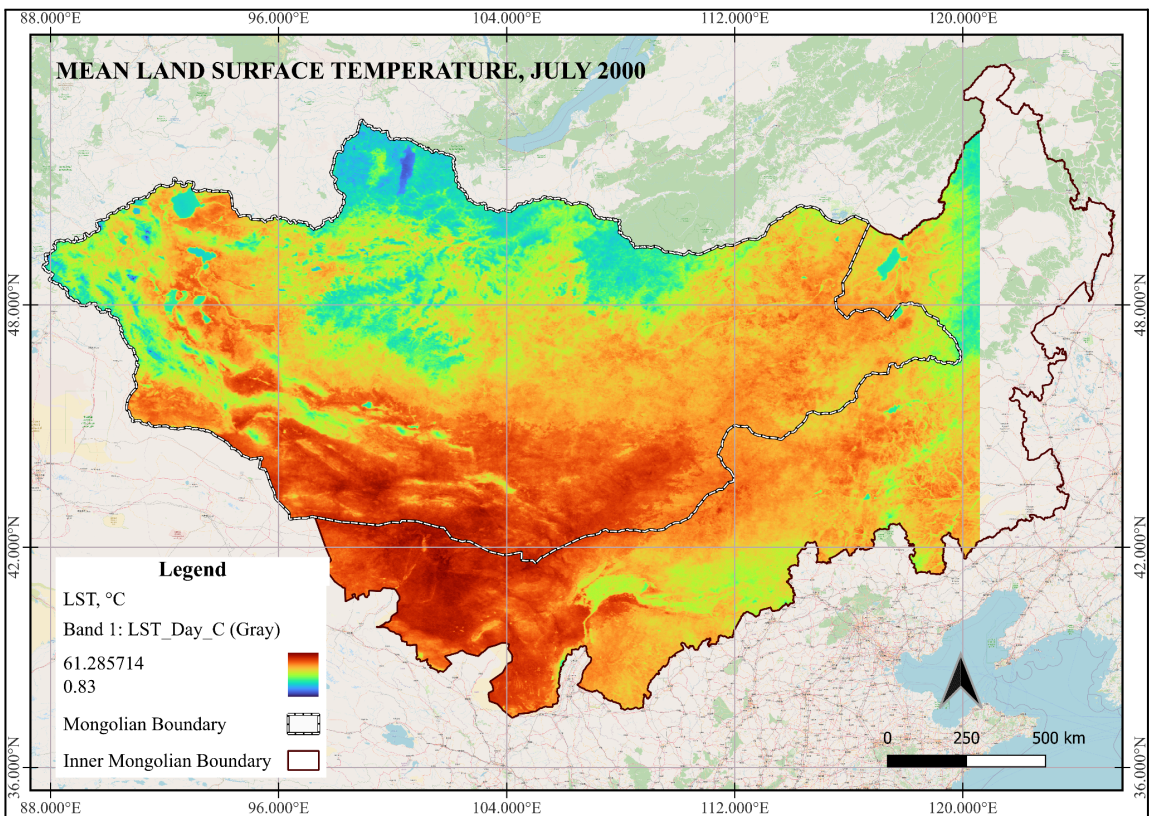


Figure 8

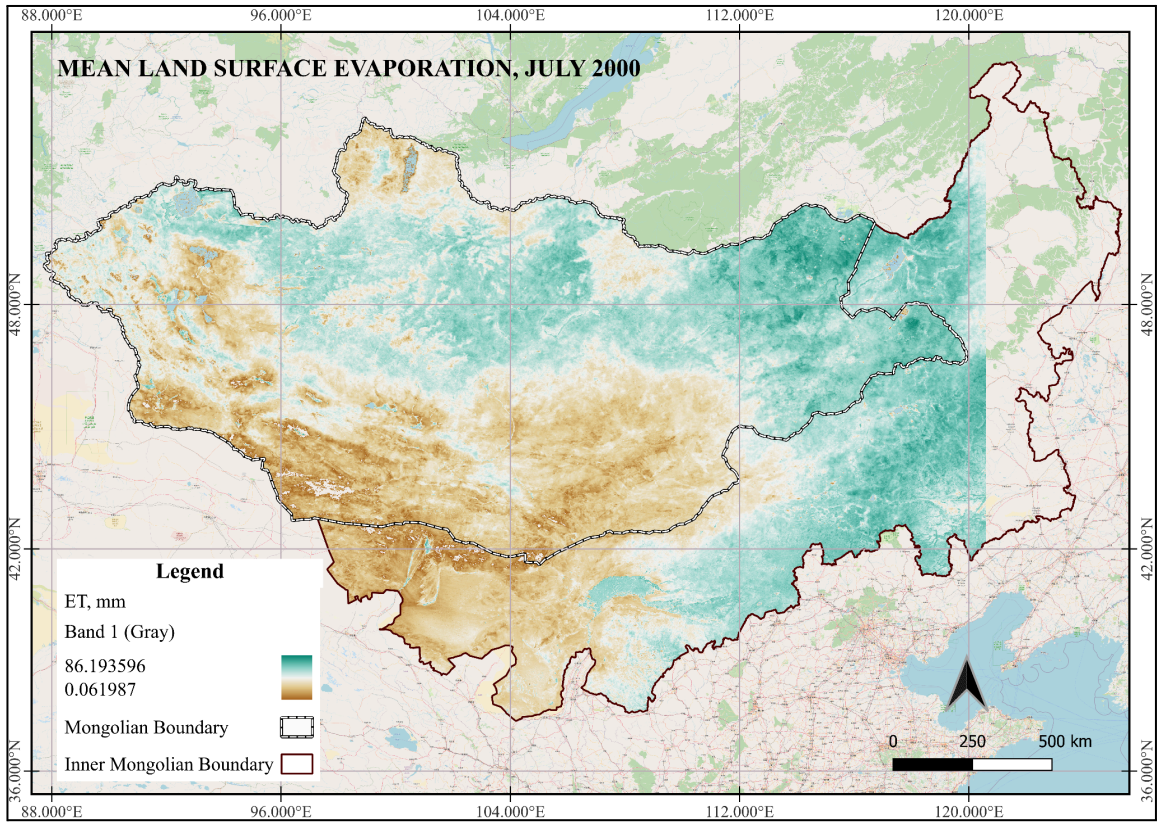


Figure 9

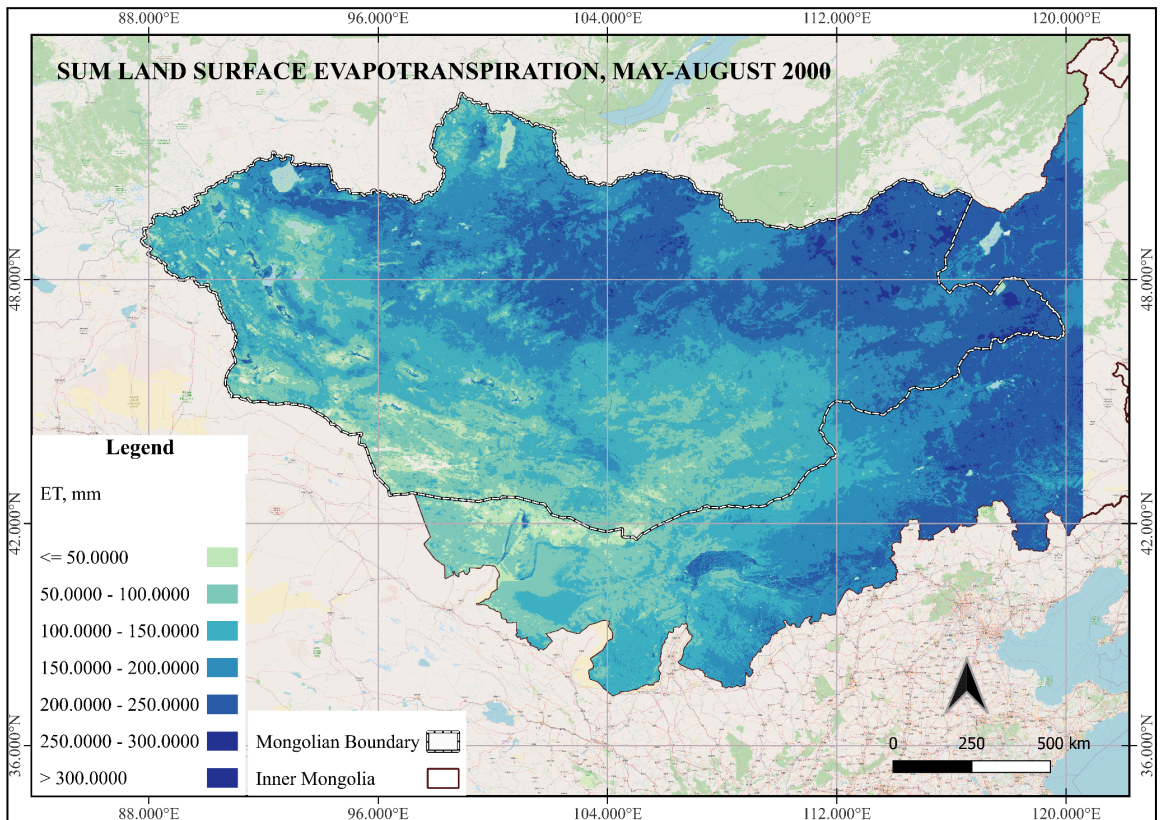


Figure 10

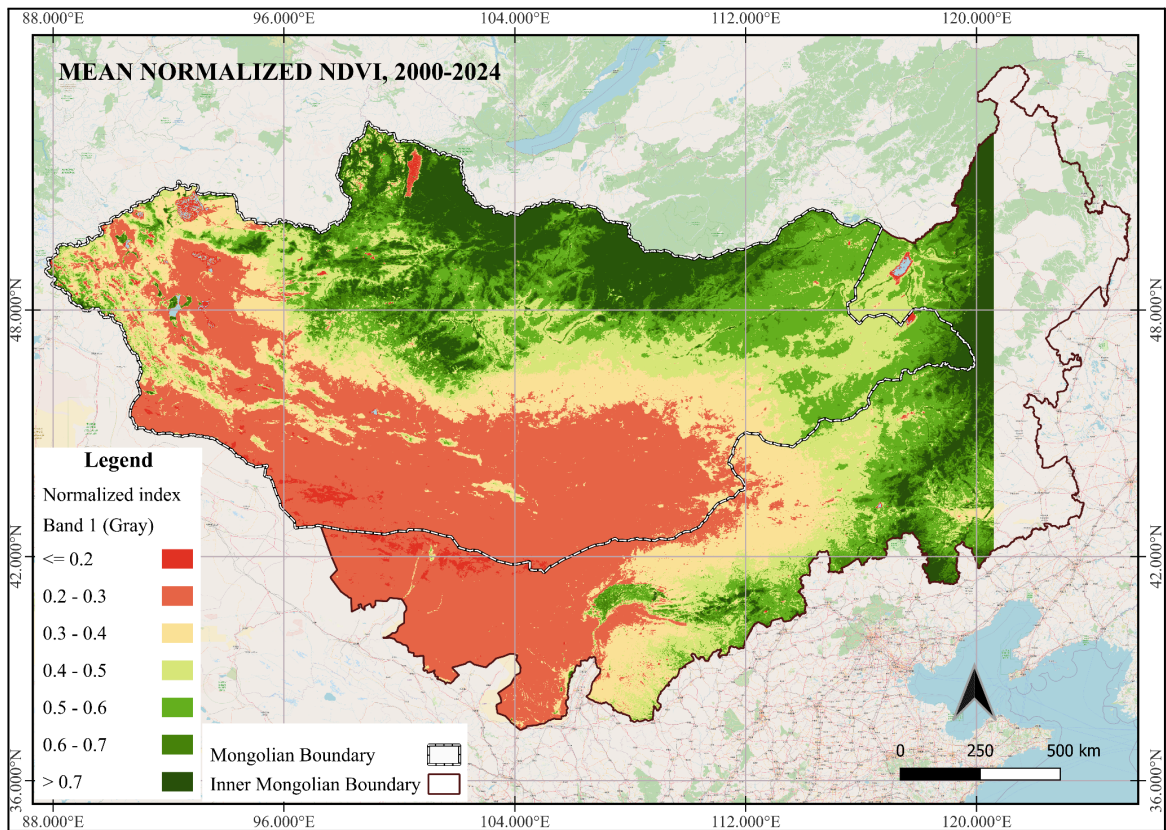


Figure 11

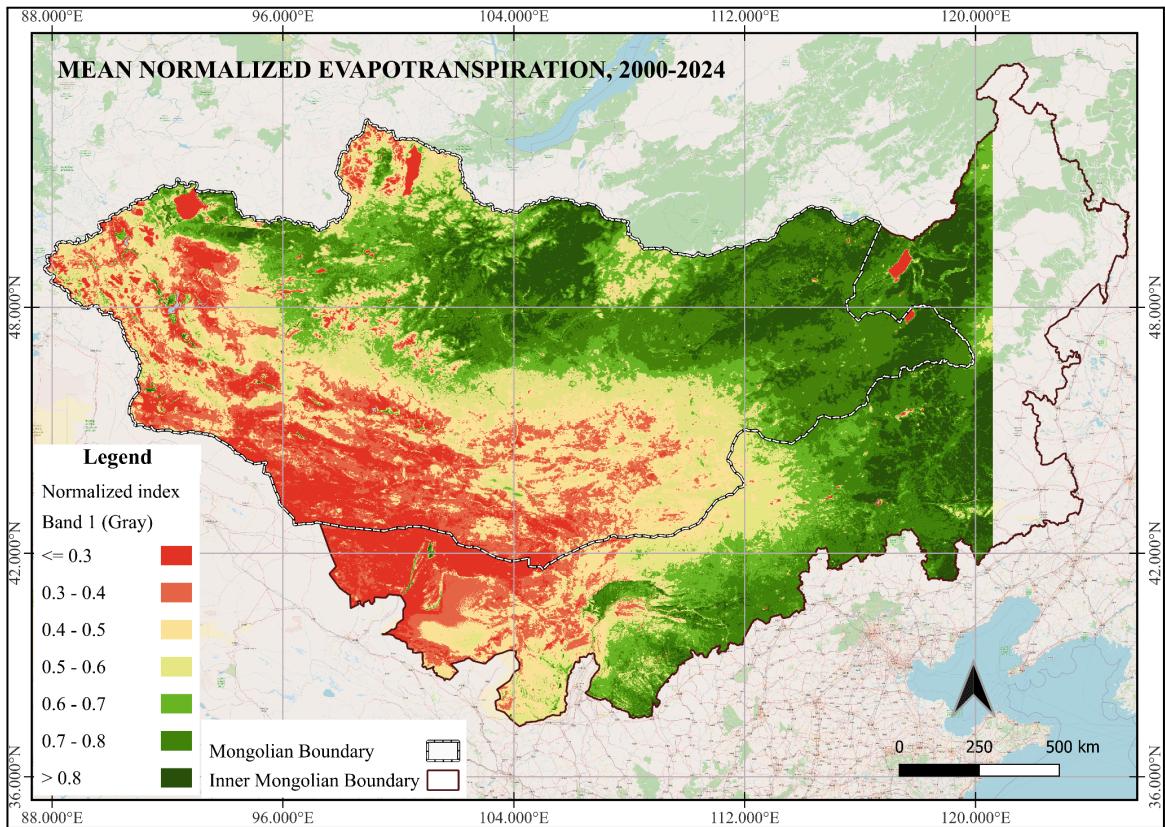


Figure 12

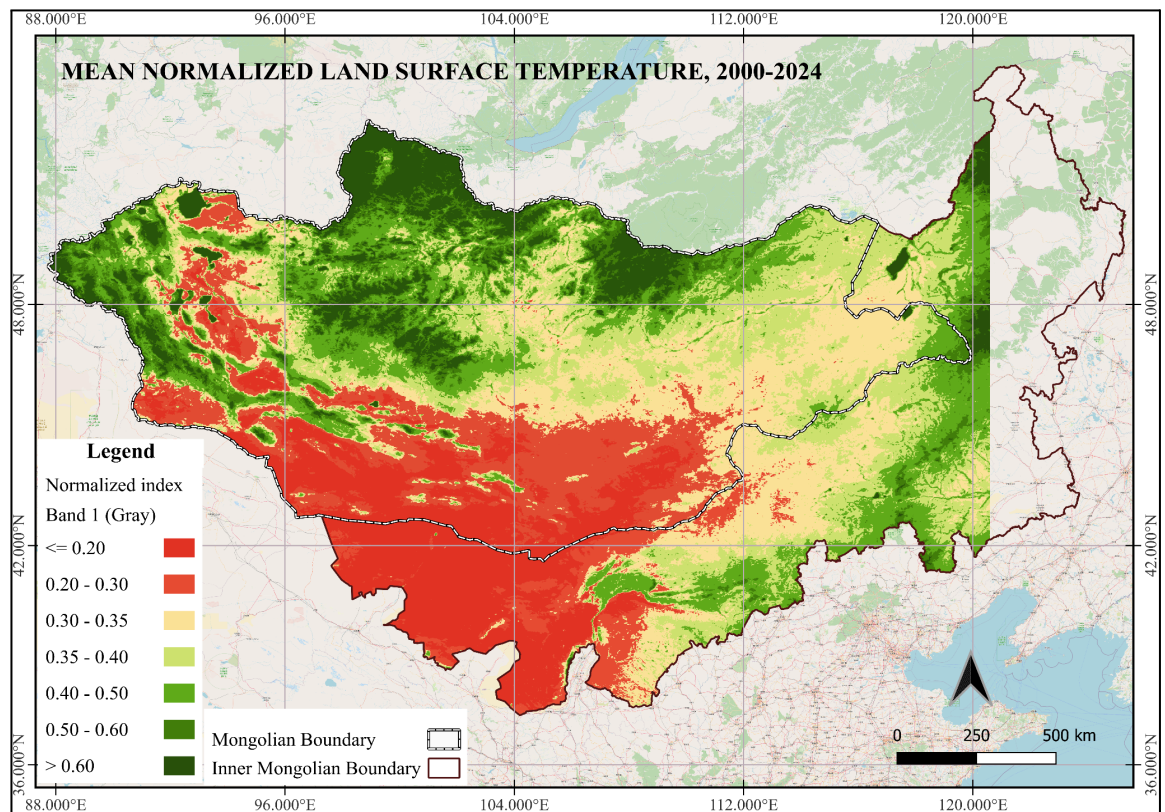


Figure 13

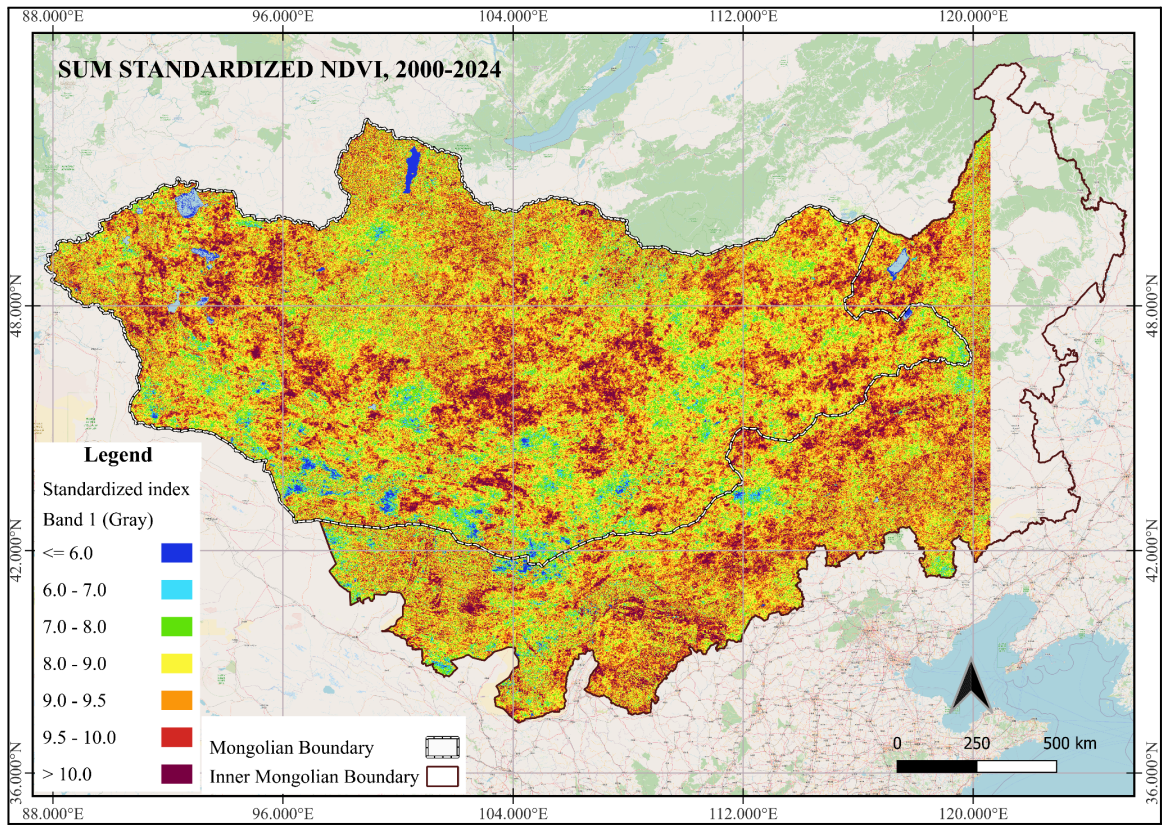


Figure 14

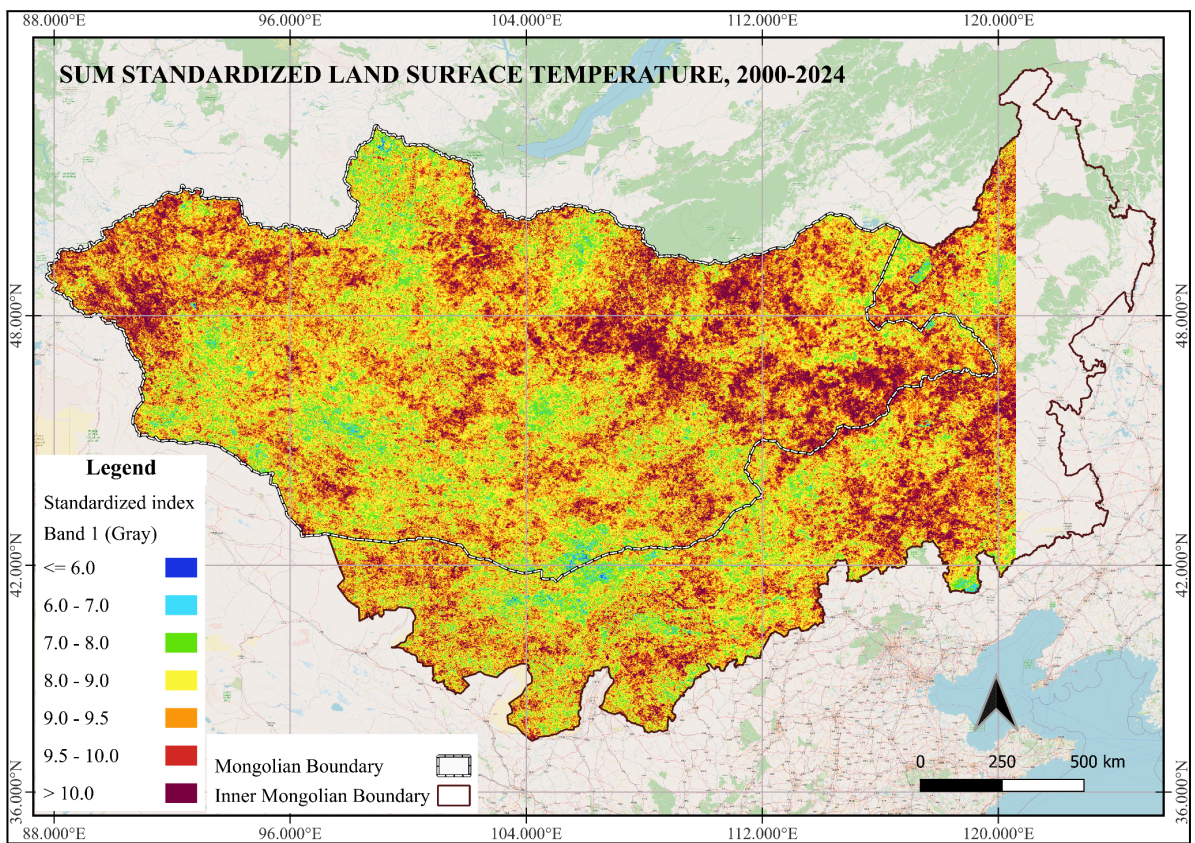


Figure 15

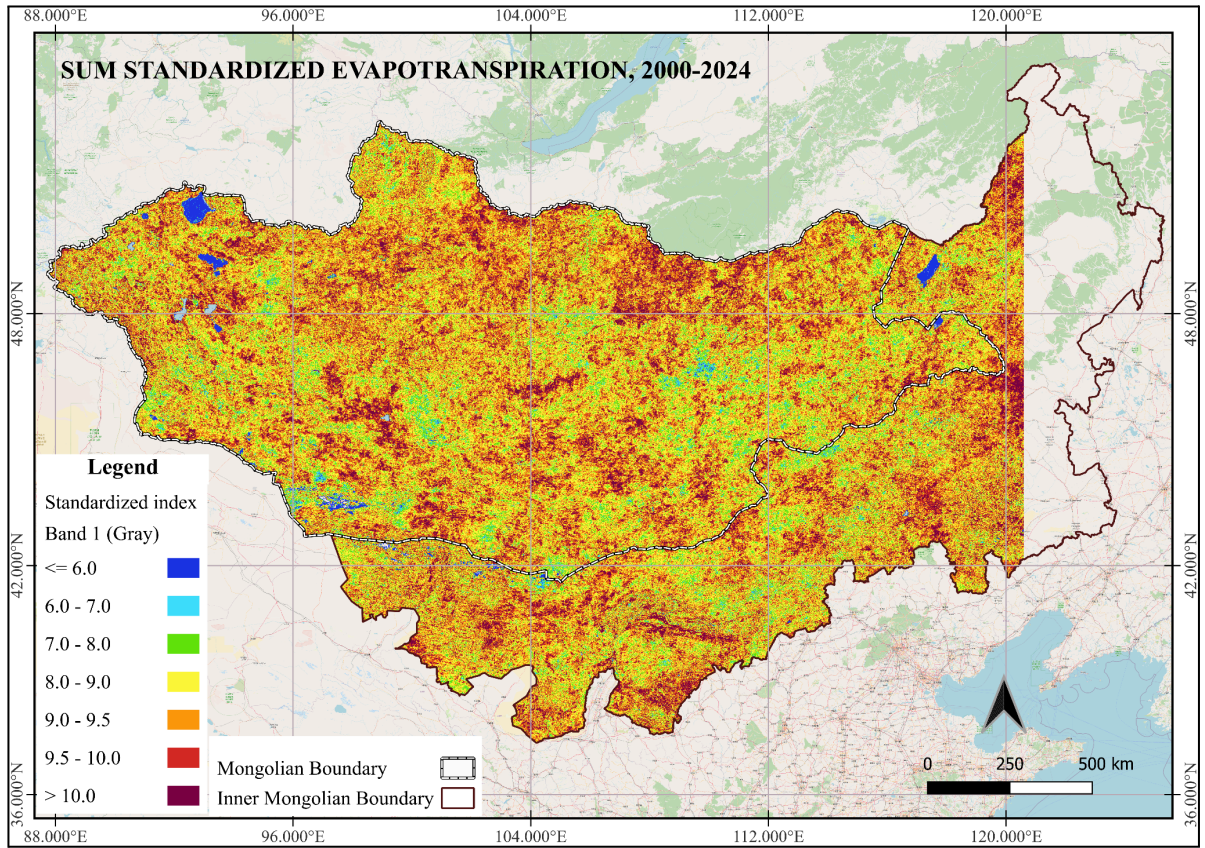


Figure 17

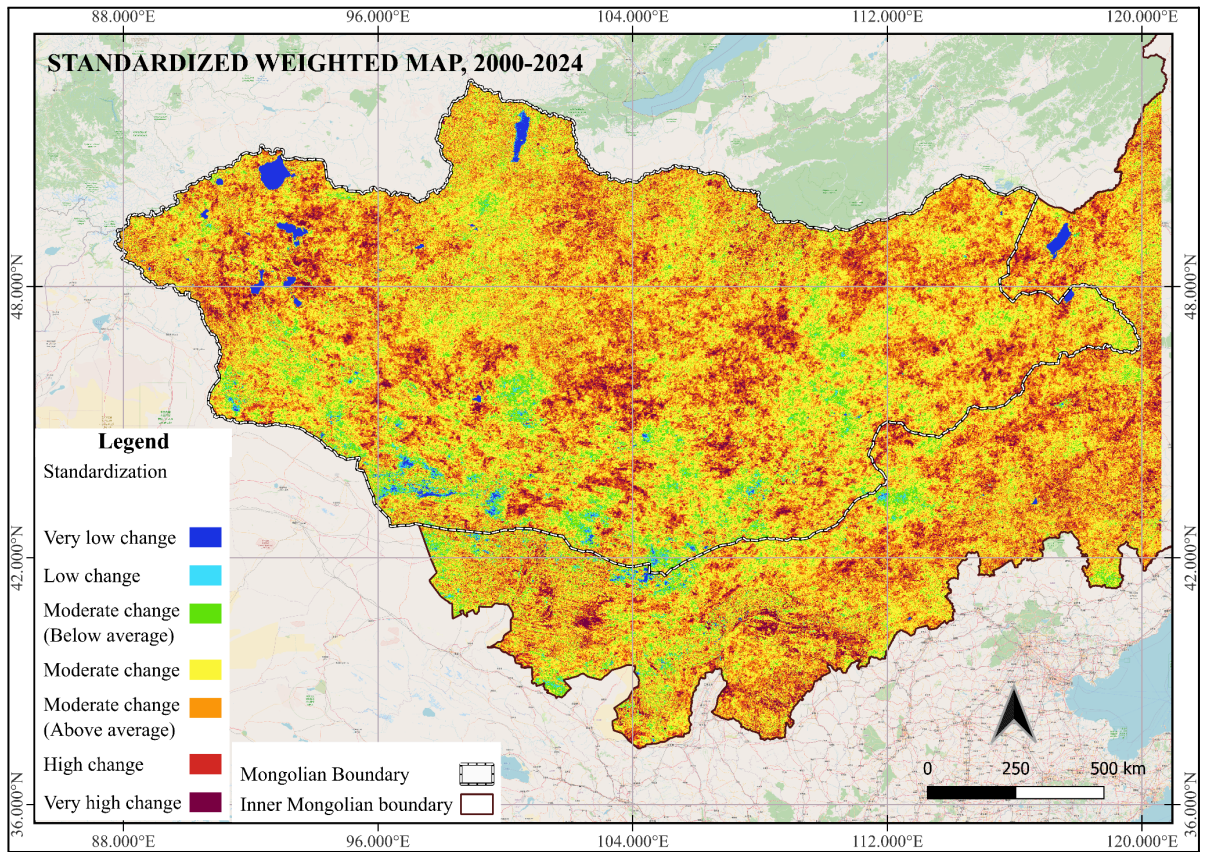


Figure 18

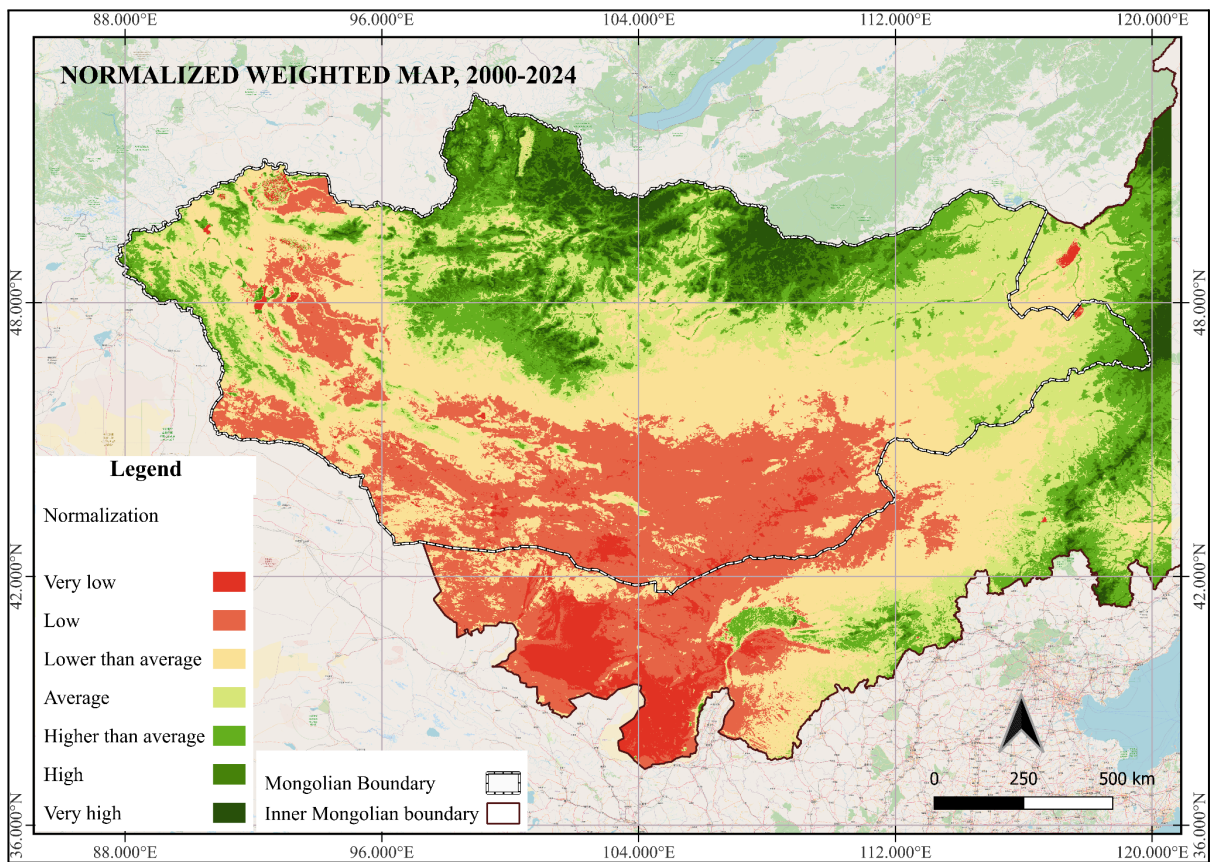


Figure 19

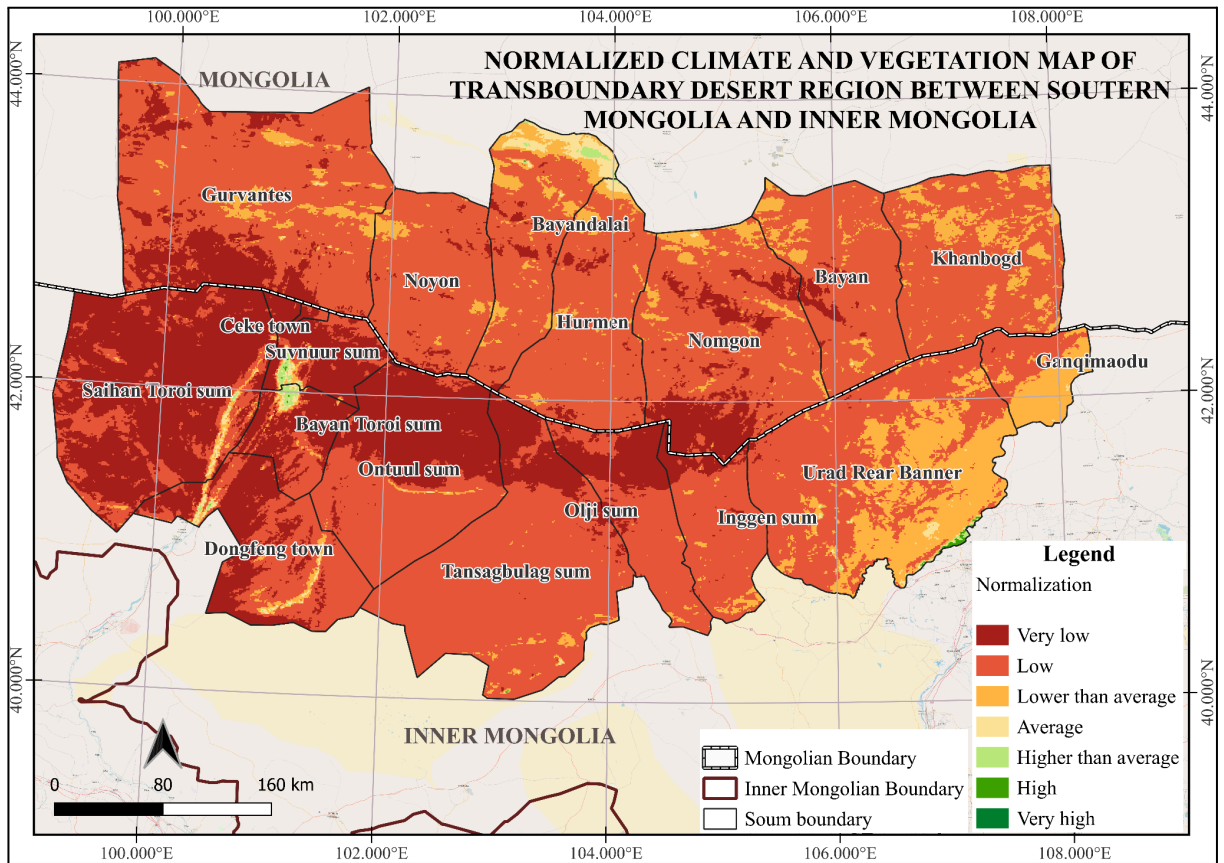


Figure 20

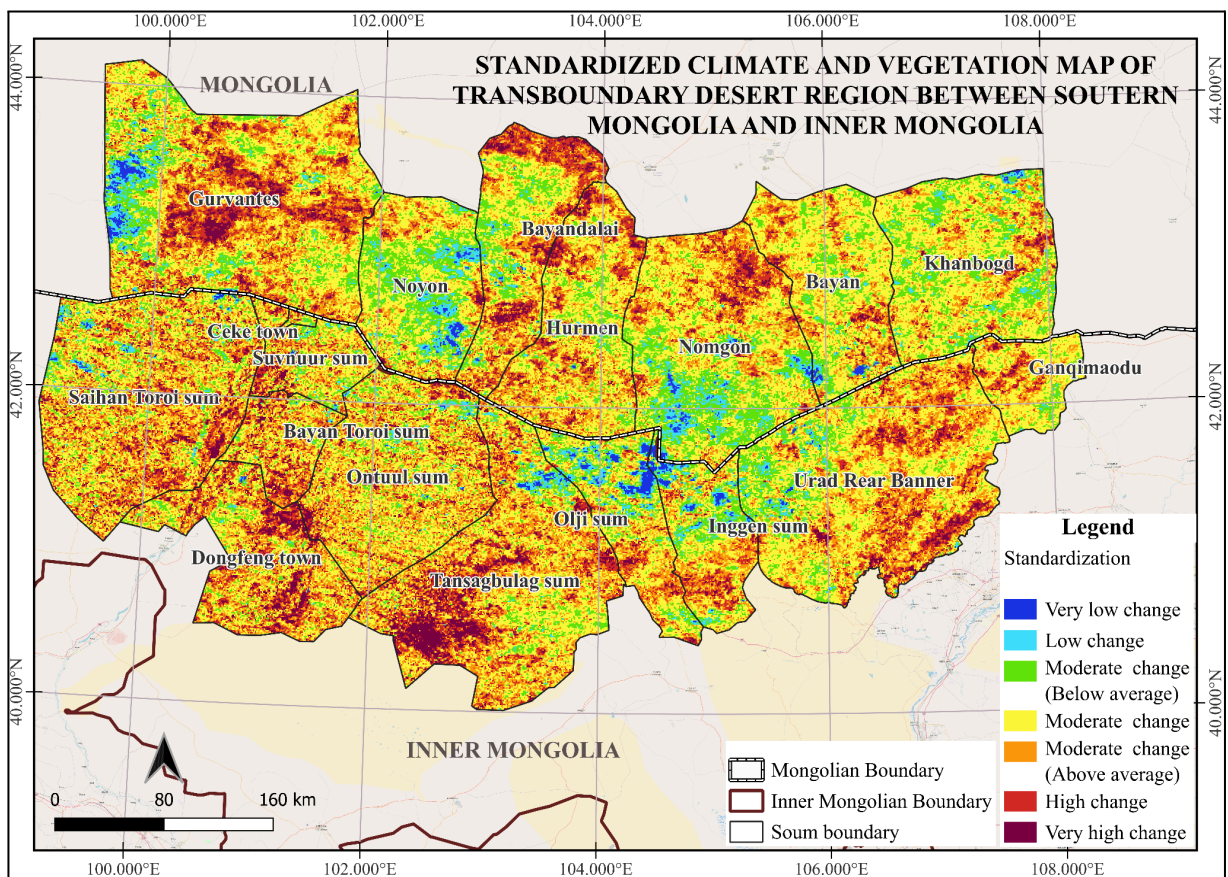


Figure 22

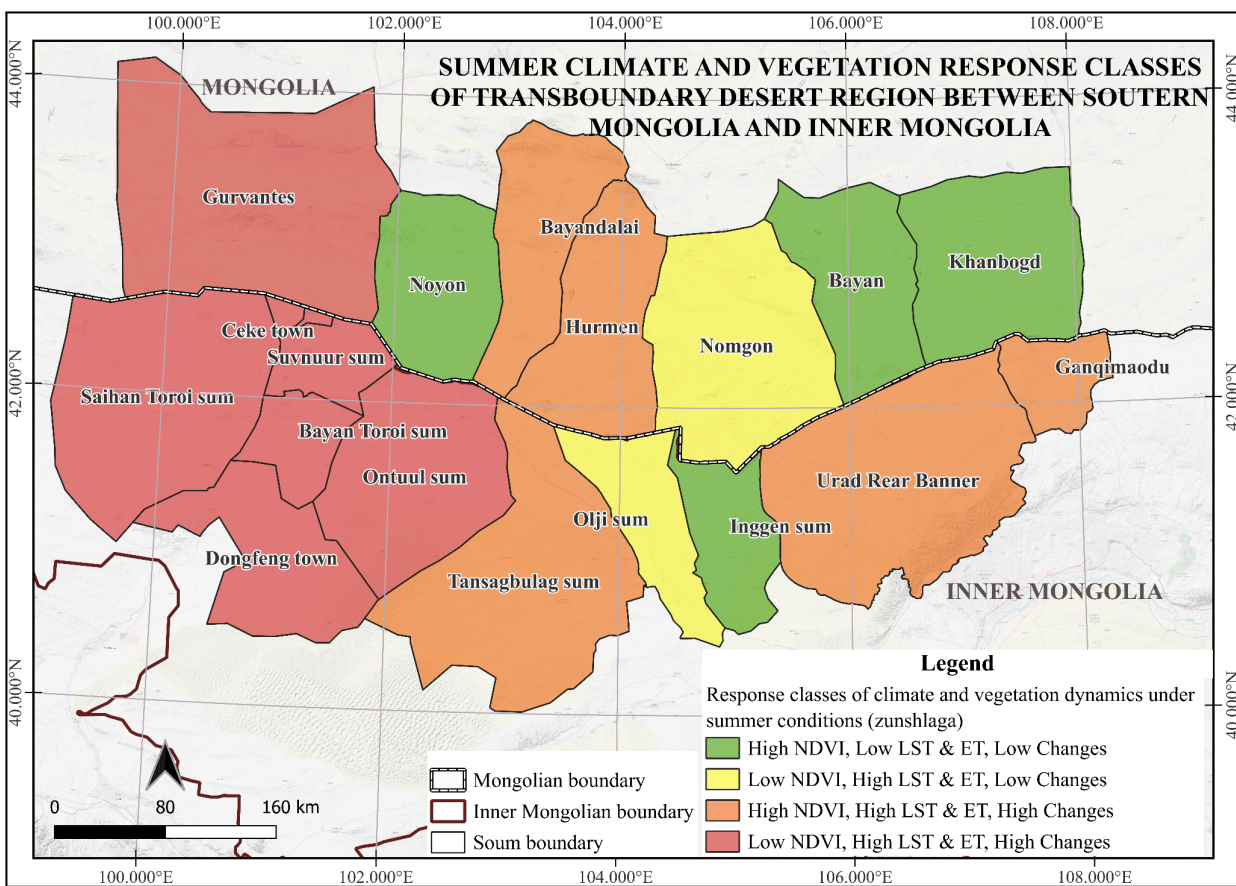


Figure 23

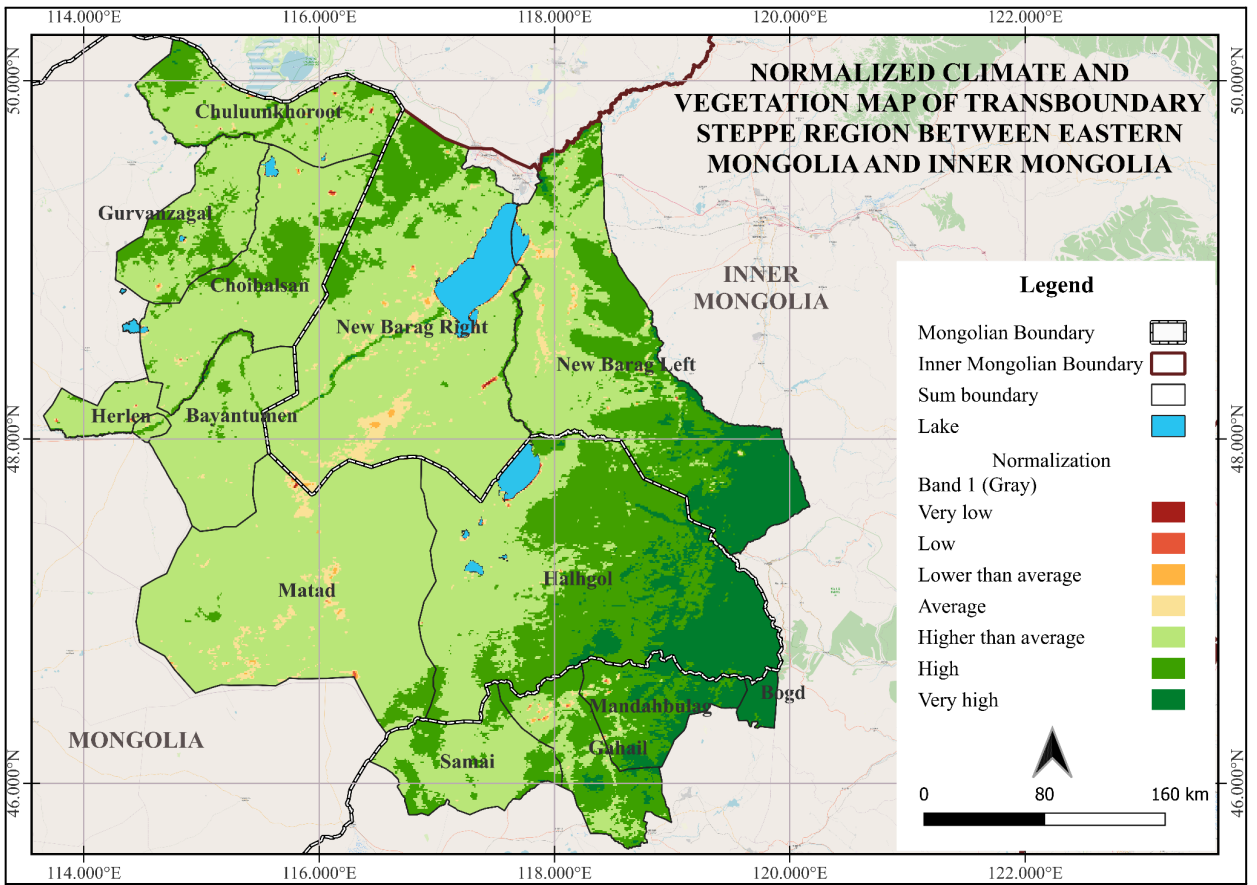


Figure 24

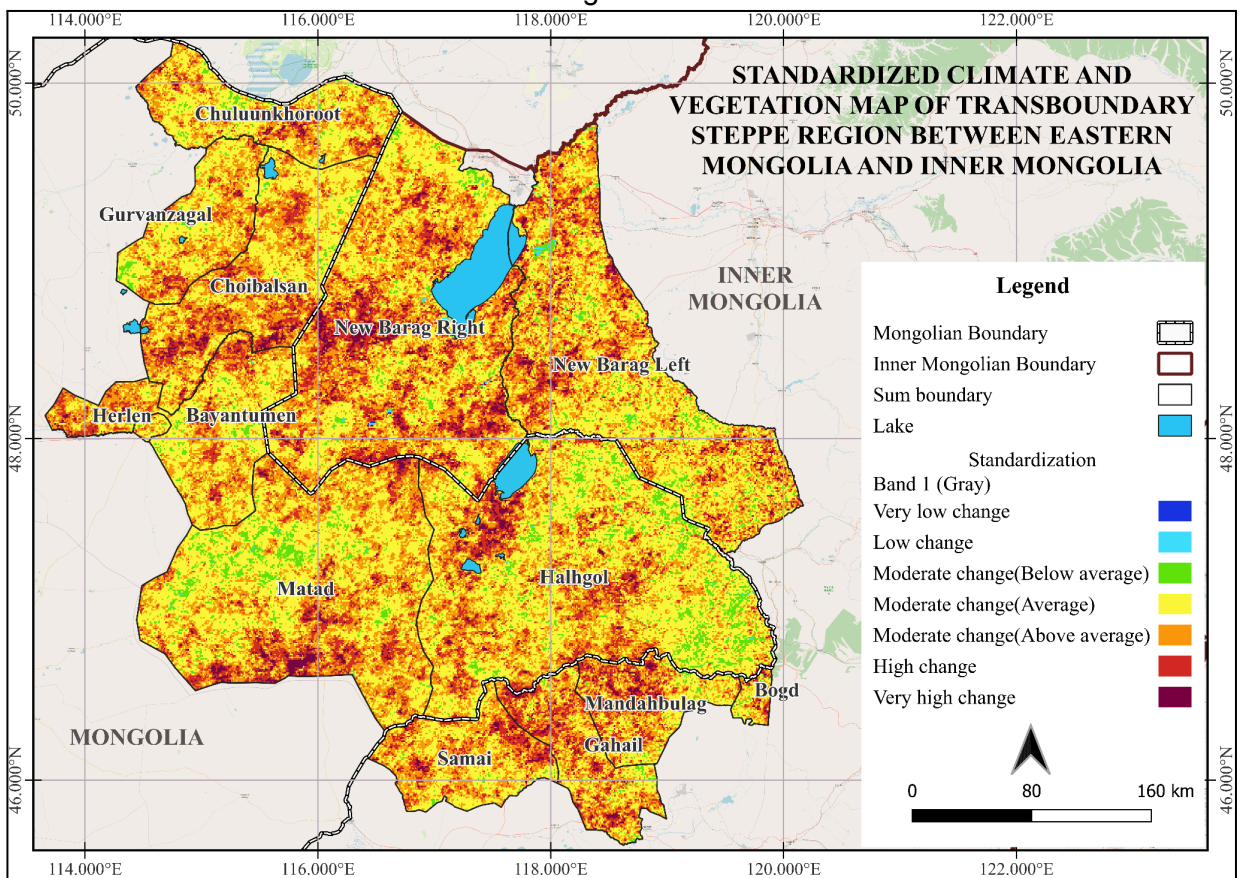


Figure 26

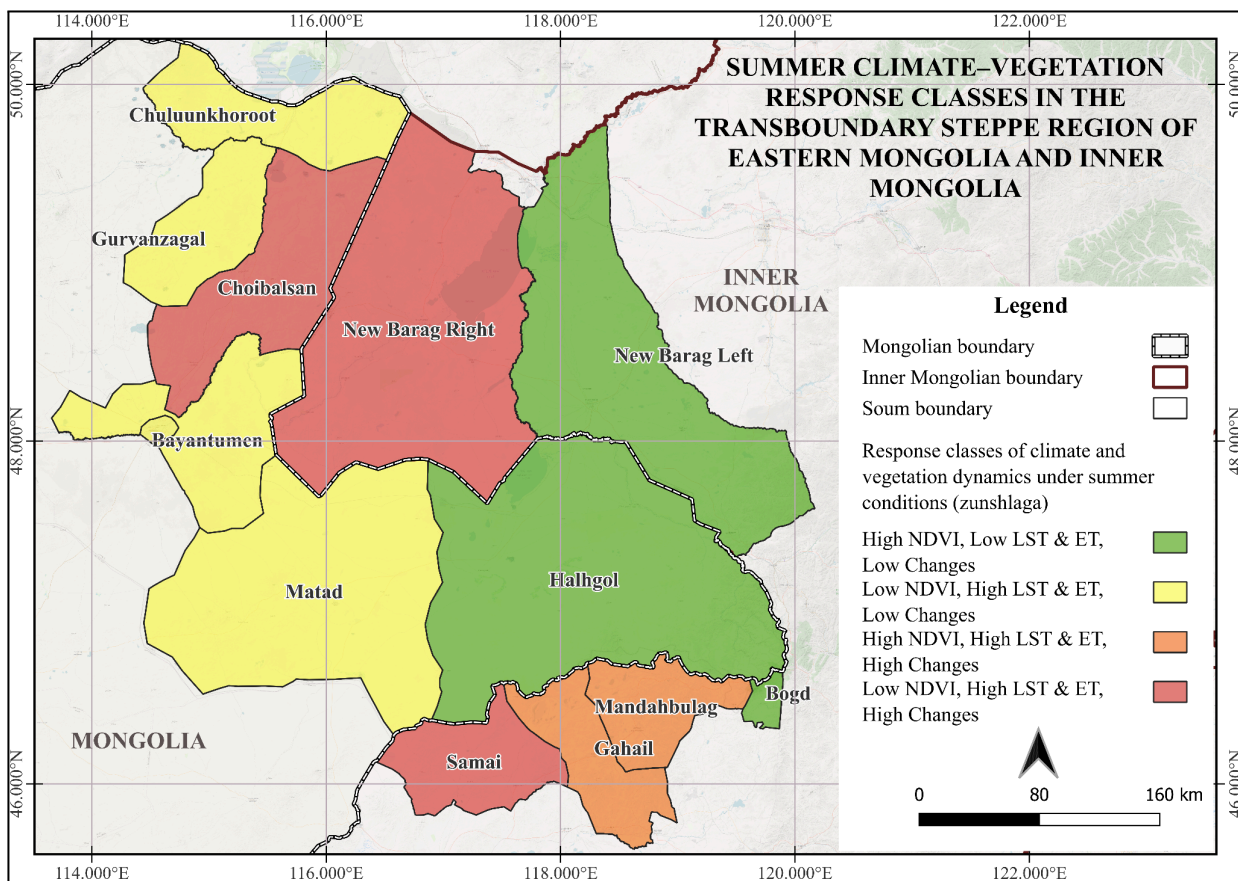


Figure 27

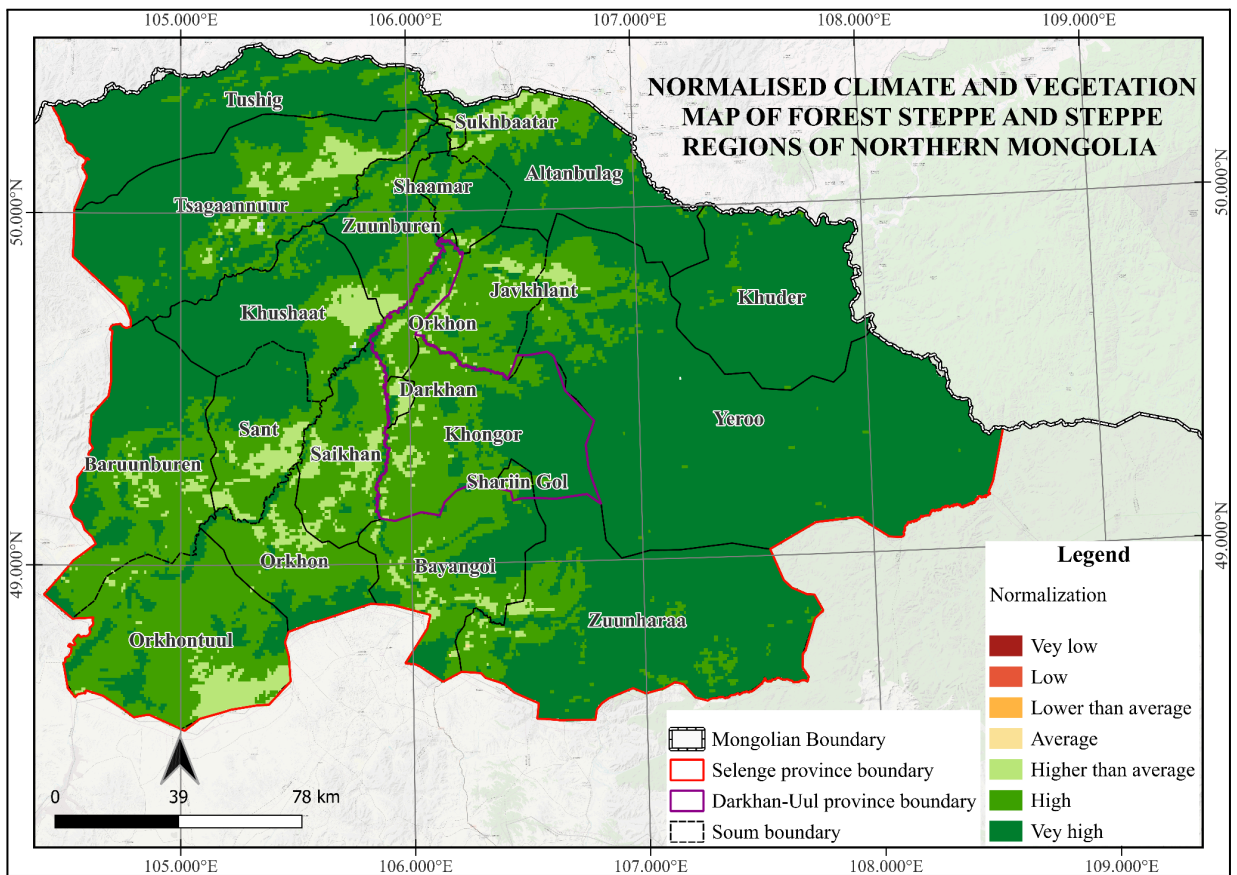


Figure 28

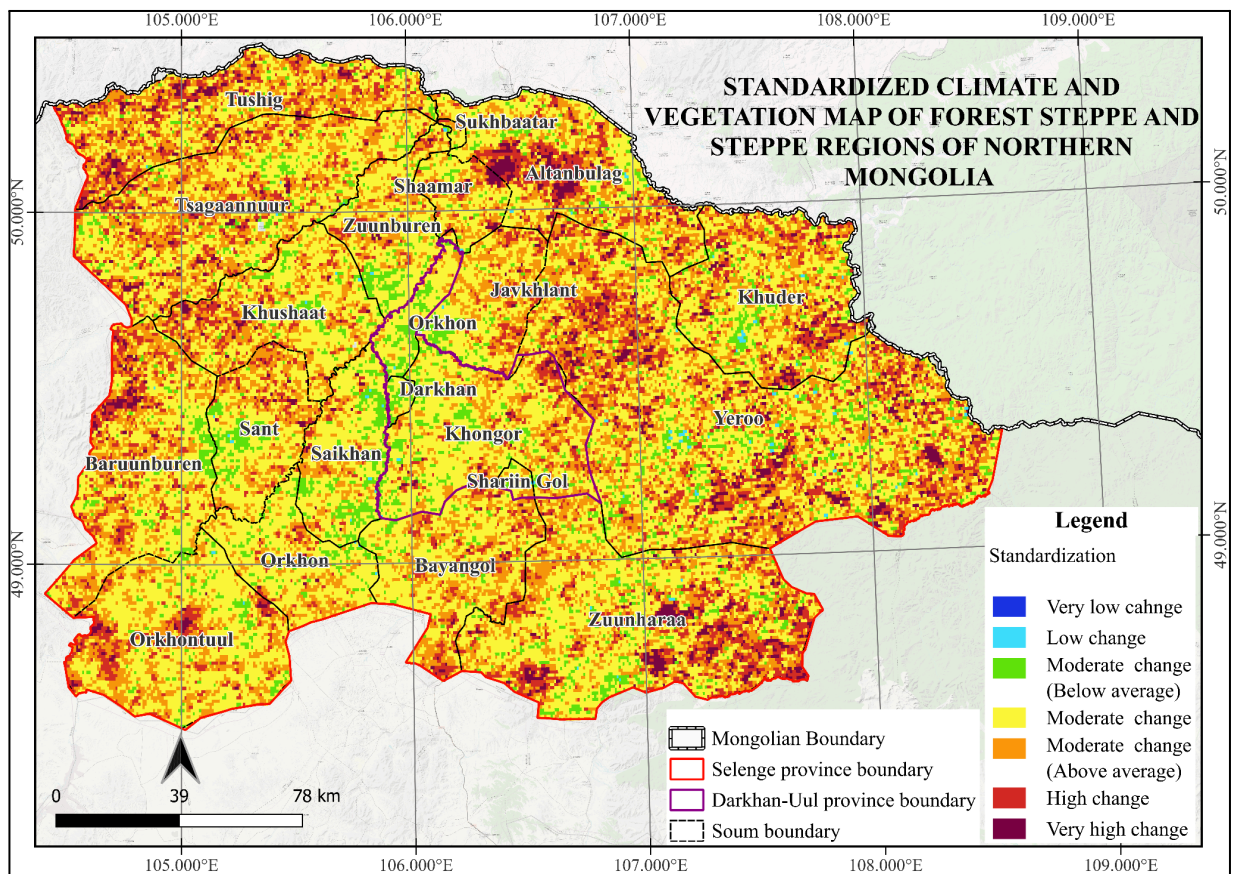


Figure 30

